FINAL REPORT

FAILURE ANALYSIS OF MULTI-LAYERED, MULTI-FUNCTIONAL COMPOSITE STRUCTURES USING A FINITE ELEMENT MULTICONTINUUM THEORY

Submitted by

Andrew C. Hansen
Department of Mechanical Engineering
University of Wyoming
Laramie, Wyoming 82071

Email:Hansen@uwyo.edu
(307)-766-3209

March 2001

Submitted to:

Yapa Rajapakse
Office of Naval Research
ONR 334
Ballston Tower One
800 North Quincy Street
Arlington, VA 22217-5660
(703) 696-4405

GRANT: N00014-97-1-1081

REPORT DOCUMENTATION PAGE

Form Approved
OMB NO. 0704-0188

1. AGENCY USE ONLY (Leave Blank)	2. REPORT DATE	3. REPORT TYPE AND DATES COVERED
	March 2001	Final 11-14-97 ; 11-14-00

4. TITLE AND SUBTITLE
Failure Analysis of Multi-layered, Multi-functional Composite Structures Using a Finite Element Multicontinuum Theory

5. FUNDING NUMBERS
N00014-97-1-1081

6. AUTHOR(S)
Andrew C. Hansen

7. PERFORMING ORGANIZATION NAME(S) AND ADDRESS(ES)
University of Wyoming
Department of Mechanical Engineering
PO Box 3295, University Station, Laramie, WY 82071

8. PERFORMING ORGANIZATION REPORT NUMBER

9. SPONSORING / MONITORING AGENCY NAME(S) AND ADDRESS(ES)
Office of Naval Research
ONR 334, Ballston Tower One
800 North Quincy Street
Arlington, VA 22217-5660

10. SPONSORING / MONITORING AGENCY REPORT NUMBER

11. SUPPLEMENTARY NOTES

12 a. DISTRIBUTION / AVAILABILITY STATEMENT
Approved for public release; distribution unlimited.

12 b. DISTRIBUTION CODE

13. ABSTRACT (Maximum 200 words)

In this report, we develop a progressive failure analysis for composite structural laminates based on constituent (phase averaged) stress fields. Damage in a composite material typically begins at the constituent level and may be limited to only one constituent in some situations. An accurate prediction of constituent failure at sampling points throughout a laminate provides a genesis for progressively analyzing damage propagation in a composite structure.

The failure analysis approach presented utilizes a classic strain decomposition to extract constituent stress and strain fields during a routine finite element analysis at the *structural* level. We refer to this approach as a Multicontinuum Theory (MCT) in recognition of the continuum nature of the constituent stress and strains. Constituent-based, quadratic, stress-interactive, failure criteria are developed to take advantage of the micro-scale information provided by MCT. The criteria are fully three-dimensional and require a minimum number of experimentally derived constants. A finite element implementation utilizing the proposed failure criteria was used to generate one-dimensional stress-strain curves and two-dimensional failure surfaces for a variety of composite laminates under uniaxial and biaxial loads. The results were shown to be superior to comparable single continuum failure analyses and in good agreement with experimentally determined failure loads.

14. SUBJECT TERMS	15. NUMBER OF PAGES
composites, failure, structural, constituent, multicontinuum	75
	16. PRICE CODE

17. SECURITY CLASSIFICATION OF REPORT	18. SECURITY CLASSIFICATION ON THIS PAGE	19. SECURITY CLASSIFICATION OF ABSTRACT	20. LIMITATION OF ABSTRACT
UNCLASSIFIED	**UNCLASSIFIED**	**UNCLASSIFIED**	**UL**

NSN 7540-01-280-5500

Standard Form 298 (Rev.2-89)
Prescribed by ANSI Std. 239-18
298-102

Administrative Information

This final report is a deliverable required under contract N00014-97-1-1081 between the Office of Naval Research and the University of Wyoming, Dr. Andrew C. Hansen, Principal Investigator. The report, as per the subject contract, addresses technical issues related to development and implementation of a finite element based failure analysis for composite structures.

I. Executive Summary

Background

A majority of structural failure criteria developed for composite materials to date can be classified as macromechanical because the criteria attempt to predict failure using composite stress-strain data. A key element of macromechanics is the combining of constituent properties into a homogeneous set of composite lamina properties and possibly combining lamina properties into homogeneous laminate properties. In contrast, micromechanical failure analyses retain the individual identities of the lamina and their constituents. Micromechanical failure models have seen limited application in structural analyses due to the difficulty in acquiring information at the constituent level.

In this research, we develop a progressive failure analysis for composite structural laminates based on constituent (phase averaged) stress fields. Damage in a composite material typically begins at the constituent level and may, in fact, be limited to only one constituent in some situations. An accurate prediction of constituent failure at sampling points throughout a laminate provides a genesis for progressively analyzing damage propagation in a composite structure. A constituent based failure model also allows one to identify intermediate damage modes.

The failure analysis approach presented utilizes the classic strain decomposition put forth by Hill to extract constituent stress and strain fields during a routine finite element analysis at the *structural* level. We refer to this approach as a Multicontinuum Theory (MCT) in recognition of the continuum nature of the constituent stress and strains. Constituent-based, quadratic, stress-interactive, failure criteria are developed to take advantage of the micro-scale information provided by MCT. The criteria are fully three-dimensional and require a minimum number of experimentally derived constants. A finite element implementation utilizing the proposed failure criteria was used to generate one-dimensional stress-strain curves and two-dimensional failure surfaces for a variety of composite laminates under uniaxial and biaxial loads. The results were shown to be superior to comparable single continuum failure analyses and in good agreement with experimentally determined failure loads.

Figure 1 shows experimentally determined biaxial failure data along with two-dimensional failure surfaces developed using MCT and the classic Tsai-Wu failure criterion. The agreement between the MCT analysis and the experimental data is excellent. We note the failure envelope of Figure 1 predicted by MCT appears to be nothing more than what a maximum stress criterion would yield. This is a fortuitous result that is attributed to biaxial testing of a $[0/90]_S$ laminate. Other stress paths produce no correlation to a maximum stress criterion.

The lack of accuracy in the Tsai-Wu predictions can be attributed to the inability to distinguish between constituent failure and total failure at a continuum point. The inability to differentiate between minor (matrix) and major (fiber) constituent damage over penalizes any simulation of a laminate's load carrying

capability. Clearly, any delineation between matrix and fiber failure is not possible for failure criteria that do not identify a failure mode. The multicontinuum failure analyses developed here-in naturally accounts for constituent failure and further provides a rigorous methodology for determining composite properties for intermediate failure states.

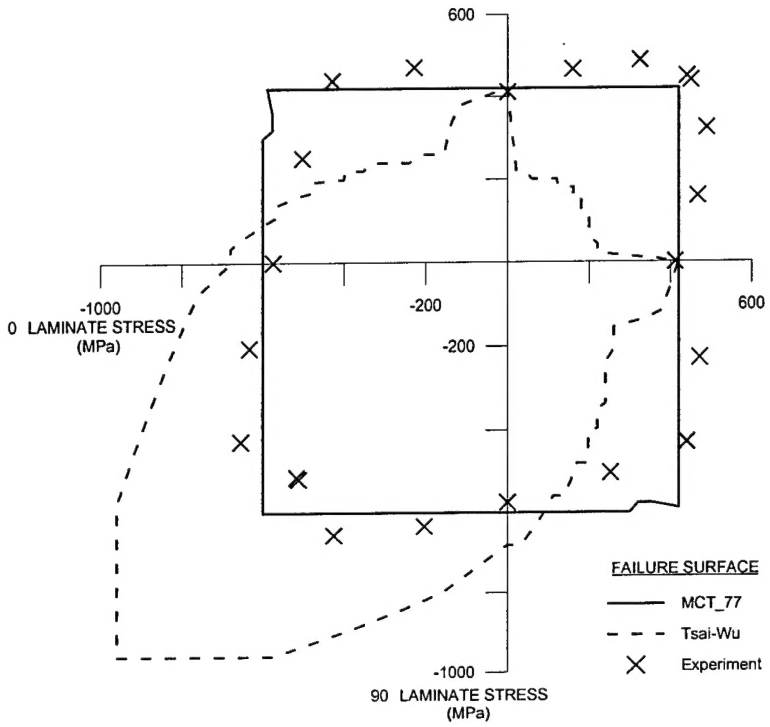

Fig. 1. *AS4/3501 [0/90]$_S$ laminate biaxial failure envelopes for combined 0-90 loading.*

Accomplishments

The overall objective of the proposed research was to *investigate the effectiveness of using constituent level data in determining composite failure.* We have met or exceeded all goals and expectations related to this objective. Specific technical milestones we have achieved are identified below.

- We have successfully implemented constituent based failure algorithms in a finite element environment. The algorithm allows a user to access constituent information, determine constituent failure, and soften the structure appropriately without a time penalty when compared to a traditional structural analysis. We have also demonstrated that constituent information significantly improves failure predictions for unidirectional laminates when compared to traditional single continuum theories.

- The original effort outlined in this proposal was directed at failure investigations for continuous fiber unidirectional composite laminates. However, the predominance of woven fabric architectures in Navy systems makes it imperative to extend the MCT technology to accommodate woven fabrics. We have accomplished this task.

To begin, we successfully developed a finite element micromechanics model for a plain weave composite material designed to simulate the microstructure of woven fabric panels fabricated by *Seemann Composites, Inc. Seemann Composites* uses the SCRIMP technology to fabricate composite panels on a large scale with near aircraft quality. The micromechanics model has been used to generate a large constituent based failure database.

We have also successfully developed a progressive failure analyses for a plain weave using the MCT technology. The model shows excellent correlation when compared with experimental data for uniaxial and shear tests. The model was also correlated to a simple structural test on angle brackets made from woven fabric panels fabricated by *Seemann Composites*. Angle brackets with two different fabric orientations were tested and analyzed using MCT. The experimental ultimate load for the two configurations varied by approximately 20 percent. In both cases, the MCT analysis predicted structural failure within 10 percent of the experimental load.

- Although not a specific task in this proposal, the MCT technology has been implemented in the commercial finite element code *ABAQUS*. Navy engineers at NSWC, Carderock are currently working with this version of ABAQUS to study failure predictions for composite structures of Navy interest.

- Two papers have been written to date on the developments of MCT related to this proposal. These papers are presented in Section II and represent the technical section of this report. The first paper in Section II is being submitted to the *Journal of* **Mechanics** *of* **Composite Materials** *and* **Structures.** The paper clearly demonstrates the value of constituent based failure predictions.

  The second paper in Section II has been accepted for publication pending 3 minor modifications as part of the **World Wide Failure Exercise** conducted by DERA, Great Britain. This exercise involved making blind predictions of failure in composites based on material properties supplied by the organizers. A second paper related to this exercise will be forthcoming in which we are given full access to the data. Differences between are original predictions and the data supplied must be explained in this work. We expect to see the data this month.

  We are in the process of preparing a third paper for publication based on failure analysis of woven fabric composites. This work is unique from our previous MCT analyses in that a weave consists of 3 constituents as opposed to two. The additional constituent results in a significant increase in the level of complexity.

- Education of graduate students was a major component of the proposal. We have graduated 3 MS students and one Ph.D. student who were supported by funds provided by this grant. The Ph.D. student is now working as an Assistant Professor and is conducting research in composite materials. Two of the three MS students have industry jobs related to the analysis of composite materials. The third MS student is working in the software industry.

  Three appendices are provided as part of this final report. These documents are essentially dissertations and theses written by students funded under this work. Appendix A addresses the implementation of MCT and subsequent failure analysis of unidirectional composites in a finite element environment. A layered brick finite element was developed for this purpose. The element can accommodate up to 100 layers in a structure. Within each layer, the constituent

(phase averaged) stress and strain fields are available to the analysts. The development of the layered brick element and implementation of constituent based failure criteria represented a fundamental task in the proposal. Appendix A has also been released as a full Navy report from the Naval Surface Warfare Center, Carderock Division (NSWCCD-65-TR-1999/15).

Appendix B was research devoted to implementing progressive failure with MCT for viscoelastic material behavior. A structural component consisting of an angle bracket was also experimentally taken to failure and analyzed analytically. Finally, Appendix C provides the details to implementing MCT for woven fabrics.

- The proposed research has provided a spin-off business for Wyoming's software industry. Specifically, an ONR/SBIR grant has provided funding to commercialize the MCT technology.

- The research conducted under this grant has provided new research opportunities in the area of dynamic analysis of composite structures as it pertains to strain rate hardening and progressive failure. We have made significant strides in developing a strain rate hardening continuum damage model that is readily embedded into MCT. We intend to integrate the strain rate hardening model into the LSDYNA-3D computational framework. LSDYNA-3D is a commercial finite element package, and standard Navy analysis tool, for problems involving dynamic loads.

II. Technical Report

The technical report presented below is provided in the form of two technical manuscripts as discussed in the executive summary.

Paper A

Multicontinuum Failure Analysis of Composite Structural Laminates

by

J. Steven Mayes[†]
Mechanical Engineering Division
Alfred University
Alfred, NY 14802
Email: mayesjs@alfred.edu
Phone: (607) 871-2058
Fax: (607) 871-

Andrew C. Hansen[‡]
Department of Mechanical Engineering
University of Wyoming
Laramie, WY 82071
Email: hansen@uwyo.edu
Phone: (307)-766-3209
Fax: (307)-766-2695

ABSTRACT: Damage in a composite typically begins at the constituent level and may, in fact, be limited to only one constituent in some situations. Accurate predictions of constituent damage at points in a laminate provide a genesis for progressively analyzing failure of a composite structure from start to finish.

In this paper, we develop an efficient constituent based failure analysis for composite structural laminates. Continuum based (phase averaged) constituent stress and strain fields are computed in a finite element environment without a computational time penalty. Constituent stress-based failure criteria are developed and used to construct a progressive failure algorithm where one constituent is allowed to fail while the other constituent remains intact, e.g. matrix cracking.

[†] Formerly of the Structures and Composites Department , Naval Surface Warfare Center, Carderock Division
[‡] Corresponding author

The proposed failure algorithm was used to predict failure of a variety of laminates under uniaxial and biaxial loads. The results were shown to be superior to comparable single continuum failure analyses and in good agreement with experimentally determined failure loads.

Introduction

The success of continuum mechanics in predicting failure in homogeneous materials is truly remarkable. Failure theories such as maximum stress, maximum strain, and maximum distortional strain energy all utilize stress and strain fields based on the continuum hypothesis. Traditional fracture mechanics also invokes the continuum assumption with great success.

The continuum definition of stress or strain is simply the volume average of the local microscopic field of interest. For instance, the average (homogenized) value used to characterize the stress tensor at a "continuum point", shown in the hypothetical micrograph of Figure 1, is derived by taking a volume average of all stresses in the region:

$$\underset{\sim}{\sigma} = \frac{1}{V}\int_D \underset{\sim}{\sigma}(\mathbf{x})\, dV \quad , \tag{1}$$

where D is the region representing the continuum point.

While the single continuum hypothesis has worked well for predicting failure in homogeneous materials, it has certainly met with less success when applied to the myriad of composite materials in use today. The chief difficulty encountered clearly stems from applying the continuum hypothesis to a material composed of two or more constituents with drastically different material properties. To counter this problem, a natural extension of a single continuum theory is to treat the material as a multicontinuum where the individual constituents are allowed to retain their identity. In the case of the continuum stress tensor, we simply extend the definition of stress in Eqn (1) down to the constituent level. In particular, for the continuum point of Figure 1, volume averaged stresses for the fibers (f) and matrix (m) may be expressed as

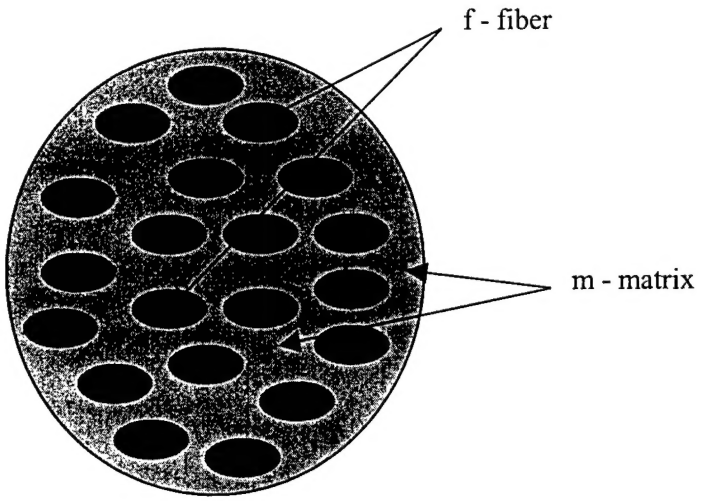

Figure 1. Macroscopic view of a continuum point with two clearly identifiable constituents.

$$\underset{\sim}{\sigma}_f = \frac{1}{V_f}\int_{D_f} \underset{\sim}{\sigma}\left(\mathbf{x}\right) dV\,, \tag{2}$$

and

$$\underset{\sim}{\sigma}_m = \frac{1}{V_m}\int_{D_m} \underset{\sim}{\sigma}\left(\mathbf{x}\right) dV\,, \tag{3}$$

where

$$D = D_f \bigcup D_m\,.$$

In this paper, we develop a progressive failure analysis for composite structural laminates based on the constituent stress fields defined by Eqn (2) and Eqn (3). The approach utilizes the classic strain decomposition put forth by Hill [1] to extract constituent stress and strain fields during a routine finite element analysis. We refer to this approach as a Multicontinuum Theory (MCT) in recognition of the coexisting continua and the phase averaged nature of the constituent stress and strain fields.

The dominant composite (macroscopic) failure criteria in use today recognize the effect of stress, or strain, component interaction on material failure. . A major contribution in this area is the work of Tsai and Wu [2] where they developed an invariant based failure theory that is quadratic in stress interaction. Although the Tsai-Wu criterion works well in many load cases, there are also many situations where difficulties arise. Again, a major source of the difficulties encountered may be traced to the presence of two constituent materials with significantly different mechanical properties.

In order to account for the uniquely different failure mechanisms occurring at the constituent level, Hashin [3] developed a three-dimensional quadratic stress interactive failure analysis that recognized two distinct and uncoupled failure modes; fiber versus matrix influenced. We adopt the view of Hashin and also develop separate failure criteria for the fiber and matrix failure modes. However, in a major departure from Hashin's work, we develop constituent failure criteria in terms of *constituent* stress fields produced by an MCT analysis. In contrast, Hashin utilized *composite* stresses for both constituent failure modes.

The difference between composite and constituent stress fields can be profound. For instance, consider a transverse tension loading of a continuous fiber unidirectional composite material where $\sigma_{22}>0$. The composite stress state is strictly one-dimensional whereas the constituent stress state is three-dimensional. Furthermore, the matrix normal stresses (σ_{11m} and σ_{33m}) in the unloaded direction are often of comparable magnitude when compared to the matrix stress (σ_{22m})in the loaded direction [4].

Clearly, for a constituent stress based failure criterion, one would expect improved failure predictions using the constituent stress fields as opposed to the composite stress fields. To verify this hypothesis, MCT failure predictions using constituent stress information are benchmarked against failure predictions using Hashin's approach as well as the Tsai-Wu failure criterion. Results show access to constituent information provided by MCT leads to improved failure predictions that are also in close agreement with experimental data.

Multicontinuum Theory

Let the composite and constituent stress fields be defined by Eqs (1)-(3).

Combining these equations leads directly to

$$\underset{\sim}{\sigma} = V_f \underset{\sim}{\sigma}_f + V_m \underset{\sim}{\sigma}_m, \tag{4}$$

where V_f and V_m are the volume fractions of fiber and matrix, respectively.

Likewise, for strains we have

$$\underset{\sim}{\varepsilon} = V_f \underset{\sim}{\varepsilon}_f + V_m \underset{\sim}{\varepsilon}_m. \tag{5}$$

We emphasize again the averaging process that results in these equations. That is, we are not concerned with stress and strain variations through individual constituents at the microscopic level but only with their phase averaged values. This is an information compromise that separates structural analysis from micromechanical analysis. Accounting for stress variations throughout individual fibers and their surrounding matrix material, even in a modest structure, is simply not possible or desirable. Finite element solutions of structural problems produce stress and strain fields of the composite, thereby providing two of the four unknowns in Eqs (4) and (5). To provide closure of the equations, constitutive relations are required for the composite as well as the constituents. Assuming elastic behavior for the composite and constituents there follows:

$$\{\sigma\} = [C](\{\varepsilon\} - \{\varepsilon_o\}), \tag{6}$$

$$\{\sigma_f\} = [C_f](\{\varepsilon_f\} - \{\varepsilon_{fo}\}), \tag{7}$$

$$\{\sigma_m\} = [C_m](\{\varepsilon_m\} - \{\varepsilon_{mo}\}), \tag{8}$$

where $[C]$ and $[C_\beta]$ represent material stiffness matrices and $\{\varepsilon_o\}$ and $\{\varepsilon_{\beta o}\}$ are thermal strains. Let the thermal strains be defined as

$$\{\varepsilon_o\} = \theta\{\alpha\}, \qquad \{\varepsilon_{fo}\} = \theta\{\alpha_f\}, \qquad \{\varepsilon_{mo}\} = \theta\{\alpha_m\},$$

where $\{\alpha\}$ represents the coefficients of thermal expansion and θ is the relative temperature. Eqs (4)-(8) can be combined to yield an expression for the constituent strain $\{\varepsilon\}$ as a function of the composite strain given by

$$\{\varepsilon_m\} = \left(V_m [1] + V_f [A]\right)^{-1} \left(\{\varepsilon\} - \theta\{a\}\right), \tag{9}$$

where

$$[A] = -\frac{V_m}{V_f}\left([C] - [C_f]\right)^{-1}\left([C] - [C_m]\right),$$

[1] is the identity matrix,

and $$\{a\} = \left([C] - [C_f]\right)^{-1}\left([C]\{\alpha\} - V_f[C_f]\{\alpha_f\} - V_m[C_m]\{\alpha_m\}\right).$$

Typically $[C_f]$, $[C_m]$, $\{\alpha_f\}$, and $\{\alpha_m\}$, are assumed known material properties of the constituents. Composite terms, $[C]$ and $\{\alpha\}$, can be developed from micromechanical modeling using the constituent values as input [4].

Substituting Eqn (9) back into (5) yields an expression for $\{\varepsilon_f\}$ as

$$\{\varepsilon_f\} = \frac{1}{V_f}\left(\{\varepsilon\} - V_m\{\varepsilon_m\}\right). \tag{10}$$

Eqs (9) and (10) allow phase averaged constituent strains to be to be calculated from composite strains at any point in the finite element model. Using Eqs. (7) and (8), constituent stresses can be calculated.

Failure Criteria

In what follows, we develop failure criteria for the constituents in a composite. It is critically important to recognize these criteria are applied at the *structural level.* As such, there are microstructural considerations which fundamentally alter one's viewpoint of constituent failure. Specifically, anisotropic failure theories must be used on seemingly isotropic matrix materials. For example, consider a transversely isotropic unidirectional composite with an isotropic matrix material. If all fibers were removed, leaving their holes, the macroscopic (*structural*) behavior of the remaining matrix material will

be transversely isotropic because of the microstructure. Furthermore, the presence of fibers as reinforcement, while altering the response of the composite, will still result in macroscopically transversely isotropic failure modes for the matrix material.

In developing constituent failure criteria for a unidirectional lamina, a local orthogonal coordinate system is defined in which the fiber axis serves as the principal, x_1, material direction, and x_2, x_3 the transverse directions. Since the material microstructure, is assumed invariant under rotations about the principal material direction, the failure state of either constituent can be expressed in terms of the following transversely isotropic stress invariants

$$\begin{aligned} I_1 &= \sigma_{11}, \\ I_2 &= \sigma_{22} + \sigma_{33}, \\ I_3 &= \sigma_{22}^2 + \sigma_{33}^2 + 2\sigma_{23}^2, \\ I_4 &= \sigma_{12}^2 + \sigma_{13}^2, \\ I_5 &= \sigma_{22}\sigma_{12}^2 + \sigma_{33}\sigma_{13}^2 + 2\sigma_{12}\sigma_{13}\sigma_{23}. \end{aligned} \tag{11}$$

A choice of a quadratic form eliminates I_5 from appearing in the failure criterion. Therefore the most general form for a quadratic criterion is

$$K_1 I_1 + L_1 I_1^2 + K_2 I_2 + L_2 I_2^2 + M_{12} I_1 I_2 + K_3 I_3 + K_4 I_4 = 1 \quad . \tag{12}$$

As discussed previously, we adopt the view of Hashin and develop separate failure criteria for the fiber and matrix failure modes. However, rather than using composite stresses to predict constituent failure, we use constituent stress fields to predict constituent failure. As a consequence, the transversely isotropic stress invariants, defined in Eqn (11), were used for each constituent in the failure criterion of Eqn (12). Furthermore, we follow the reasoning of Hashin [3] and recognize that a composite typically has different ultimate strengths in tension and compression, so both fiber and matrix failure criteria have tensile and compressive subforms. Hence, the lead coefficients in Eqn (12) are functions of only tension or compression strengths resulting in a continuous but not smooth failure surface in stress space.

Finally, we simplify Eqn (12) by setting the normal stress interaction term M_{12} to zero based on the work of Pipes and Cole [5] and Narayanaswami [6]. Tsai and Wu [2] suggest the linear terms in Eqn (12) are necessary to account for internal stresses. Internal (constituent level) stresses are accounted for in the formulation of Multicontinuum Theory so the linear terms are also eliminated from Eqn (12). Therefore, the general form for a stress interactive failure criterion, after changing to a consistent coefficient notation, is given by

$$K_1 I_1^2 + K_2 I_2^2 + K_3 I_3 + K_4 I_4 = 1. \tag{13}$$

Developing a form of Eqn (13) for fiber failure, we note that the majority of fibers used for composite reinforcement have greater transverse strengths than the matrices commonly used in conjunction with them. Hence, we assume that transverse failure of these composites is matrix dominated. Based on this assumption, we set K_2 and K_3 equal to zero in Eqn (13) as their associated stress invariants involve transverse normal stresses. The fiber failure criterion reduces to:

$$K_{1f} I_{1f}^2 + K_{4f} I_{4f} = 1. \tag{14}$$

We note the effect of neglecting terms involving K_{2f} and K_{3f} could be revisited should failure predictions prove to be inadequate.

To determine K_{1f} and K_{4f}, we solve Eqn (14) considering individual load cases of pure in-plane shear, tension, and compression. Let S_{ijf} and S_{ijm} denote failure strengths of the fiber and matrix constituents, respectively. We further delineate between tension and compression ultimate strengths using a + or - superscript.

For the case of in-plane shear load only ($\sigma_{11f} = 0$), we find

$$K_{4f} = \frac{1}{S_{12f}^2},$$

where S_{12f} denotes the fiber shear stress at failure.

For the case of tensile load only ($\sigma_{11f} > 0$; $\sigma_{12f} = 0$), we find

$$^{+}K_{1f} = \frac{1}{^{+}S_{11f}^{2}}.$$

For the case of compression load only ($\sigma_{11f} < 0$; $\sigma_{12f} = 0$), we find

$$^{-}K_{1f} = \frac{1}{^{-}S_{11f}^{2}}.$$

The criterion for fiber failure can now be expressed as:

$$^{\pm}K_{1f} I_{1f}^{2} + K_{4f} I_{4f} = 1. \tag{15}$$

The ± symbol indicates that the appropriate tensile or compressive ultimate strength value is used depending on the constituent's stress state.

To determine the coefficients of Eqn (13) for matrix failure we first solve the equation considering load cases of pure in-plane and transverse shear. For the case of transverse shear only ($\sigma_{11m}=\sigma_{22m}=\sigma_{33m}=\sigma_{12m}=0$), we find

$$K_{3m} = \frac{1}{2S_{23m}^{2}}.$$

For the case of in-plane shear only ($\sigma_{11m}=\sigma_{22m}=\sigma_{33m}=\sigma_{23m}=0$), we find

$$K_{4m} = \frac{1}{S_{12m}^{2}}.$$

Noting that a majority of fibers used for composite reinforcement have greater longitudinal strengths than the matrices commonly used in conjunction with them, we assume that the longitudinal failure of these composites is fiber dominated. Based on this assumption (and some numerical sensitivity studies) we set K_{1m} equal to zero. Incorporating these results into Eqn (13) gives

$$K_{2m} I_{2m}^{2} + \frac{1}{2S_{23m}^{2}} I_{3m} + \frac{1}{S_{12m}^{2}} I_{4m} = 1. \tag{16}$$

To determine K_{2m}, we consider the case of transverse tensile load only ($\sigma_{23m}=\sigma_{12m}=0$; $(\sigma_{22m}+\sigma_{33m}) > 0$) and find

$$ {}^{+}K_{2m} = \frac{1}{\left({}^{+}S_{22m} + {}^{+22}S_{33m}\right)^2}\left(1 - \frac{{}^{+}S_{22m}^2 + {}^{+22}S_{33m}^2}{2S_{23m}^2}\right). $$

For the constituent strength parameters, the subscript is the component of stress at failure while the superscript is the direction of ultimate applied load, e.g., ${}^{+22}S_{33m}$ is the *33* strength parameter when an ultimate tensile load is applied in the x_2 direction. Care must be taken not to interpret ${}^{+22}S_{33m}$ as an ultimate transverse strength in the x_3 direction as there is no external load in this direction.

For the case of a pure transverse compressive load ($\sigma_{23m}=\sigma_{12m}=0$; $(\sigma_{22m}+\sigma_{33m}) < 0$)

$$ {}^{-}K_{2m} = \frac{1}{\left({}^{-}S_{22m} + {}^{-22}S_{33m}\right)^2}\left(1 - \frac{{}^{-}S_{22m}^2 + {}^{-22}S_{33m}^2}{2S_{23m}^2}\right). $$

The criterion for matrix failure can now be expressed as

$$ {}^{\pm}K_{2m}I_{2m}^2 + K_{3m}I_{3m} + K_{4m}I_{4m} = 1. \qquad (17) $$

The MCT failure criteria defined by Eqs (15) and (17) require determining seven failure parameters, ${}^{\pm}K_{1f}$, K_{4f}, ${}^{\pm}K_{2m}$, K_{3m}, and K_{4m}. These parameters are functions of constituent strengths, ${}^{\pm}S_{11f}$, S_{12f}, ${}^{\pm}S_{22m}$, ${}^{\pm22}S_{33m}$, S_{12m}, and S_{23m}. *Constituent* strength parameters are derived from experimentally determined composite values. The link establishing a relationship between composite (macro) and constituent (micro) strengths is a finite element micromechanics model for a continuous fiber unidirectional composite. The finite element micromechanics model used in this research is based on an assumption of uniform hexagonal fiber packing within the lamina's matrix (Figure 2).

Determining which constituent precipitates composite failure is necessary for establishing accurate constituent failure values. Identifying the constituent that precipitates failure in longitudinal and transverse lamina tension and compression tests is intuitive and straightforward, i.e., fiber failure for longitudinal loads and matrix failure for transverse loads. Identifying the constituent leading to shear failure is more problematic as non-catastrophic matrix damage begins well before ultimate composite

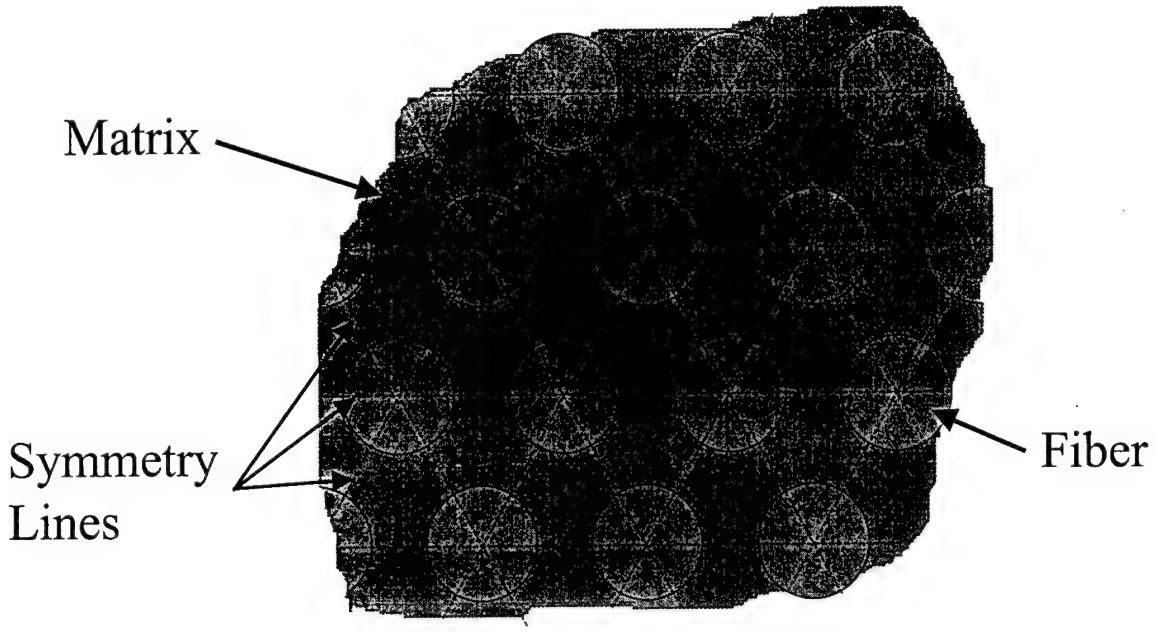

Figure 2. Hexagonal packing for a continuous fiber unidirectional composite.

strengths are reached. The reader is referred to Mayes [7] for details behind determining constituent failure strengths in shear.

The Failure Algorithm

The failure theory outlined above was implemented within the framework of a conventional finite element analysis, thereby providing a vehicle for progressive failure analysis of composite laminates. The analysis utilizes a nonlinear-elastic constitutive model developed by Mayes [7] that allowed for nonlinear shear behavior while assuming linear behavior for tensile and compressive loads.

The nonlinear character of the analysis requires the load to be incrementally applied. The composite material damage state at every Gauss point in the finite element model is stored for the entire analysis. Initially, composite material properties are set to an undamaged condition. At each load step a damage algorithm, using the failure criteria formulated in Eqs (15) and (17), checks each Gauss point for

constituent failure based on cumulative stresses. If constituent failure is detected, the corresponding moduli are reduced to a near zero value. (Near zero values are used rather than zero to avoid numerical difficulties.) We emphasize that since both intact and failed constituent properties are known *a priori,* micromechanics can be used to determine damaged composite properties due to a failed constituent *outside* the MCT program and prior to a structural analysis.

When constituent failure is detected at a Gauss point, stresses are recalculated using accumulated strains and updated material properties. Gradual softening of the structure due to constituent material failure and the nonlinear-elastic constitutive model causes an equilibrium imbalance between the applied (external) and internal load vectors. A standard Modified Newton-Raphson nonlinear iterative procedure within each load is used to achieve equilibrium prior to the next load step.

Comparison of Analysis Versus Experiment

In this section, results from MCT failure analyses are compared against experimental data of laminates fabricated from two different materials and tested under uniaxial and biaxial load conditions. The first material studied consisted of E-glass/ vinylester (Dow 8084) laminates fabricated by *Seemann Composites, Inc.* The second material consisted of carbon/epoxy (AS4/Hercules 3501-6) laminates fabricated by the Composite Materials Research Group at the University of Wyoming. Experimentally determined elastic constants and failure parameters for the composite and the constituents for both materials are given in Tables 1-5 [7].

Stress-strain curves are used to qualify MCT's ability to simulate laminate structural behavior. Over twenty stress-strain plots are presented in Mayes [7]. We present a single plot here that brings out the salient features of the analysis. Specifically, Figure 3 shows the stress-strain response for a quasi-isotropic $[0/\pm45/90]_S$ E-glass/vinylester laminate under uniaxial tension. The figure shows MCT stress-strain predictions incorporating constituent failure as well as a linear elastic prediction. The introduction of constituent failure is clearly necessary to simulate the stress-strain response. Matrix tensile failure

occurred analytically in the 90° plies at approximately 80 MPa. Later in the load history, a combination of tensile and shear stresses matrix failure in the ±45° plies was predicted by MCT prior to catastrophic tensile fiber failure in the 0° plies. Ultimate failure loads were within 13% of the experimental value.

MCT failure predictions are benchmarked against Hashin's failure analysis for a variety of E-glass/vinylester and carbon/epoxy laminates. When constituent failure is determined using either approach, the corresponding failed composite properties are reduced in an identical manner according to finite element micromechanics analyses conducted previously. The intent of this exercise is to isolate the effect of using *constituent* information provided by MCT. Specifically, does constituent stress information result in improved predictive capability for failure of composite materials when compared to comparable failure criteria that utilize composite stress information? Finally, failure predictions

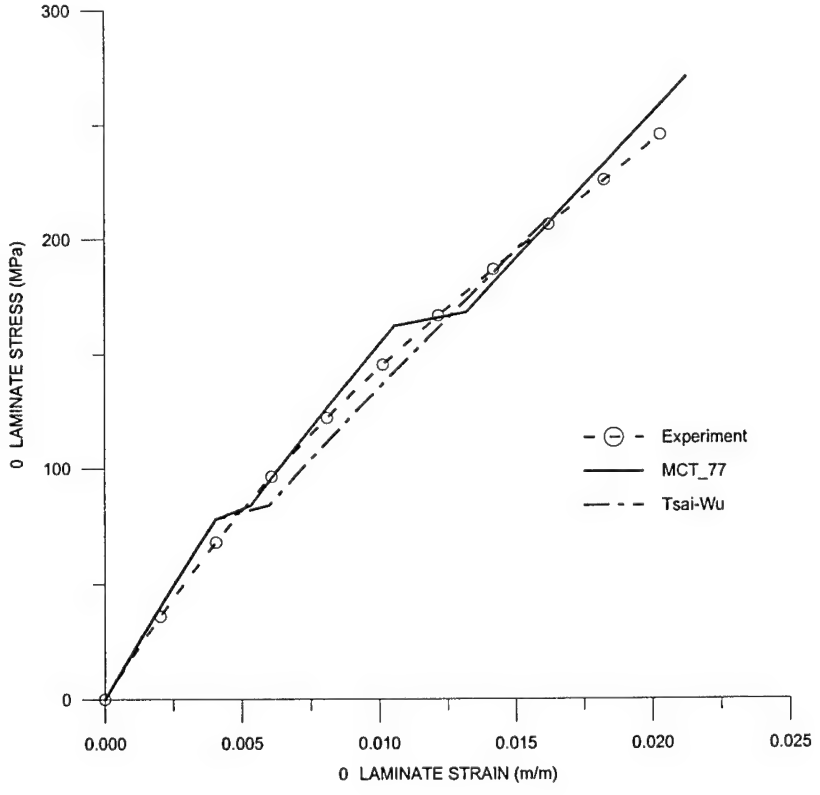

Figure 3. E-glass/vinylester $[0/90/\pm45]_S$ laminate under uniaxial tension.

Composite	E_{11} (GPa)	E_{22} (GPa)	G_{12} (GPa)	G_{23} (Gpa)	ν_{12}	FVF
AS4/3501	134.0	9.14	7.29	3.16	0.261	0.66
E-glass/8084	38.5	11.7	4.74	4.34	0.273	0.51

Table 1. Composite elastic constants derived from experimental data.

Constituent	E_{11} (GPa)	E_{22} (GPa)	G_{12} (GPa)	G_{23} (GPa)	ν_{12}	ν_{23}
AS4 carbon	201.0	13.5	95.0	4.90	0.22	0.25
3501-6 epoxy	4.30	4.30	1.59	1.59	0.35	0.35
E-glass	71.0	71.0	28.2	28.2	0.260	0.260
8084 vinylester	4.66	4.66	1.80	1.80	0.292	0.292

Table 2. In situ elastic constants for constituents.

Composite	${}^{+}S_{11}$ (MPa)	${}^{-}S_{11}$ (MPa)	${}^{+}S_{22}$ (MPa)	${}^{-}S_{22}$ (MPa)	S_{12} (MPa)	S_{23} (MPa)
AS4/3501-6	1335.	-1992.	28.0	-282.	115.	33.0
E-glass/8084	818.	-760.	45.3	-144.3	60.8	48.5

Table 3. Composite ultimate strengths.

Fiber	${}^{+}S_{11}$ (MPa)	${}^{-}S_{11}$ (MPa)	${}^{+}S_{22}$ (MPa)	${}^{-}S_{22}$ (MPa)	S_{12} (MPa)	S_{23} (MPa)
AS4	1335.	-1992.	28.	-282.	115.	33.
E-glass	1507.	-1399.	1507.	-1399.	120.	120.

Table 4. In situ fiber strengths.

Matrix	${}^{+}S_{22}^{22m}$ (MPa)	${}^{-}S_{22}^{22m}$ (MPa)	${}^{+}S_{33}^{22m}$ (MPa)	${}^{-}S_{33}^{22m}$ (MPa)	S_{12}^{12m} (MPa)	S_{23}^{23m} (MPa)
3501-6	22.6	-228.	-3.63	36.7	45.1	25.0
8084	37.1	-118.	2.20	-7.04	34.4	25.2

Table 5. In situ matrix strengths.

using the popular Tsai-Wu criterion are included for completeness. It should be noted that the Tsai-Wu stress interaction terms were set to zero.

Table 6 compares MCT, Hashin, and Tsai-Wu failure predictions for E-glass/vinylester laminates. A metric of predictive accuracy or "modeling bias" (predicted/experimental values) shows all theories performed respectably although MCT produced significantly less scatter overall as measured by the coefficient of variation (COV = standard deviation/mean average). A comparison of the two constituent based failure criteria shows the MCT algorithm predicted failure within 10 % of the experimental load in 12 of 13 cases. In contrast, the Hashin criterion was within 10 % on 8 of 13 cases considered.

Failure data for laminate specimens fabricated from carbon/epoxy (AS4/ Hercules 3501-6) composites are summarized in Table 7. In comparing the constituent based criteria, the COV for MCT and Hashin theories was 14.3% and 19.8 %, respectively. A close inspection of the table shows that, in general, MCT failure predictions were significantly closer to experimental values than those produced using Hashin's. The Tsai-Wu criterion faired considerably worse than either of the constituent based failure criteria.

Arguments can be made that most composite structures typically operate under multi-axial load states. Therefore, testing composite laminates under such conditions would be the prudent course of action. Unfortunately, triaxial or biaxial load tests of composite laminates are considerably more difficult to accomplish than uniaxial load tests. As a result, there is a paucity of multi-axial experimental failure data to verify analysis. Welsh [8] designed and fabricated a triaxial test frame and experimentally developed biaxial (tension-tension and tension-compression) failure surfaces for carbon/epoxy $[0/90]_S$ laminates. The experimentally determined biaxial failure data along with two dimensional failure surfaces developed using MCT and Tsai-Wu failure criteria are shown in Figure 4.
Hashin's criterion is not shown since, for this simple laminate configuration, no discernable difference between the two constituent based failure criteria would appear. The failure surface generated

Eglass/8084 Laminate	Exp	MCT/Exp	Tsai-Wu/Exp	Hashin/Exp
[0/90]S	-381	1.01	1.01	1.01
[0/90]S	374	1.03	1.11	1.10
[0/90/±45]S	-301	0.95	0.79	0.96
[0/90/±45]S	245	1.13	0.88	1.13
[±45]S	-110	0.95	0.98	1.00
[±45]S	100	0.96	1.05	1.10
[5]N	537	1.09	1.01	1.01
[10]N	281	1.05	1.12	1.14
[15]N	187	1.04	1.12	1.18
[20]N	140	1.06	1.11	1.21
[30]N	93	1.06	1.10	1.20
[45]N	67	1.04	1.04	1.10
[60]N	53	1.06	1.02	1.04
	Avg =	1.03	1.03	1.09
	COV =	5.1%	9.6%	7.5%

Table 6. Summary of failure loads for E-glass/vinylester laminates.

AS4/3501 Laminate	Exp	MCT/Exp	Tsai-Wu/Exp	Hashin/Exp
[±15]S	786	1.40	2.80	1.41
[±22]S	786	1.01	2.02	1.06
[±30]S	455	1.00	2.05	1.11
[±45]S	155	0.95	1.08	1.32
[±60]S	-288	0.97	1.14	1.22
[±60]S	74	1.16	0.73	0.74
[±75]S	43	1.02	0.77	0.77
[90/0]3S	-1074	1.01	1.26	1.01
[(±45/02)2/90]	-1074	1.03	0.67	0.98
[±45/0/90]2S	-855	0.91	0.69	0.91
[±452/03/±45]S	-827	0.94	0.44	0.97
[±452/03/902]S	-746	1.22	0.97	1.23
[±452/90/0]S	-753	0.83	0.53	0.80
[±452/903/02]S	-599	1.20	1.02	1.20
	Avg =	1.05	1.15	1.05
	COV =	14.3%	58.8%	19.8%

Table 7. Summary of failure loads for AS4/3501 laminates.

by the MCT failure criterion and the experimental data were in excellent agreement whereas the failure surface generated by Tsai-Wu failure criterion was not.

The lack of accuracy in the Tsai-Wu predictions can be attributed to the inability of the criterion to distinguish between constituent failure and total failure at a continuum point. The inability of the Tsai-Wu criterion to differentiate between minor (matrix) and major (fiber) constituent damage over penalizes any simulation of a laminate's load carrying capability. As noted in Hashin [3], it is essential to know how a material has failed in a progressive finite element analysis. Clearly, this is not possible when a criterion predicts failure without identifying a failure mode. However, MCT naturally accounts for fiber versus matrix failure states.

The failure envelope of Figure 4 predicted by MCT appears to be nothing more than what a maximum stress criterion would yield. This is a fortuitous result that is attributed to biaxial testing of a $[0/90]_S$ laminate. Other stress paths produce no correlation to a maximum stress criterion. For instance, Figure 5 shows a biaxial failure surface for a $[0/90]_S$ laminate under combined in-plane shear and normal loading. Interestingly, Tsai-Wu and MCT failure predictions produced near identical results.

Summary

Constituent (phase averaged) stress and strain fields open a new and manageable information window for failure analysis of composite structures. The work presented herein demonstrates that this information adds value in the form of improved failure predictions when compared to comparable single continuum approaches. Furthermore, this additional information is readily accessed in a finite element environment with no computational penalty. Appropriate changes to the composite stiffness matrix due to constituent failure are also accommodated in a rigorous and logical manner.

Finally, although the composite laminates tested as part of this research effort were under one or two-dimensional loading, the constituents experienced a full three-dimensional stress state. The successful failure predictions presented herein were based on MCT failure criteria that used the full

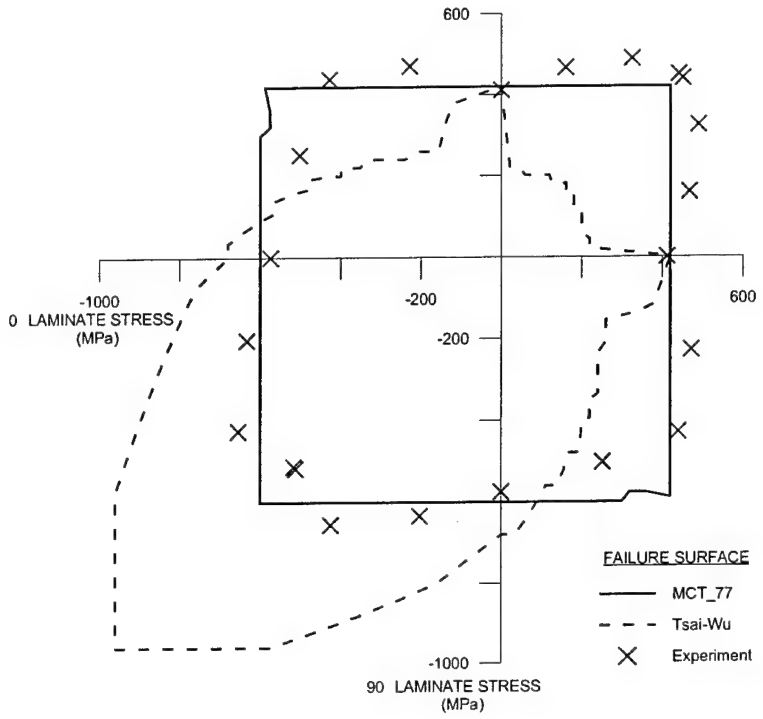

Figure 4. AS4/3501 $[0/90]_S$ laminate biaxial failure envelopes for combined 0-90 loading.

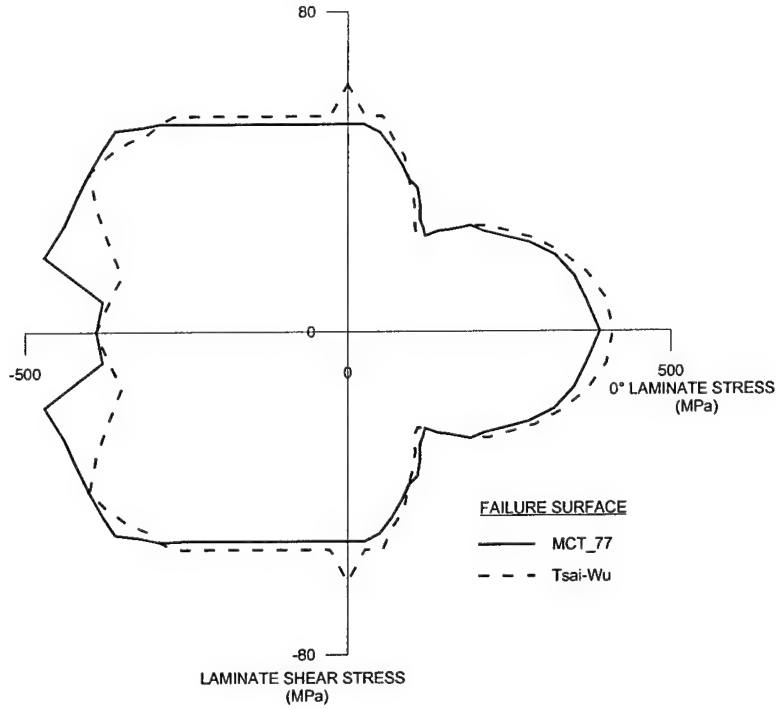

Figure 5. E-glass/vinylester $[0/90]_S$ laminate biaxial failure envelopes for combined 0-shear loading.

three-dimensional constituent stress fields. Hence, there is good reason to believe that an MCT approach will also be successful in predicting material failure in general composite structures under arbitrary three-dimensional loading.

Acknowledgements

This research was supported by the Office of Naval Research (Grant: N00014-97-1-1081), the Naval Surface Warfare Center, Carderock Division (Grant: N00167-97-1502) and by the In-house Laboratory, Independent Research program at the Naval Surface Warfare Center, Carderock Division.

References

1. Hill, R. "Elastic Properties of Reinforced Solids: Some Theoretical Principles," *J. Mech. Phys. Solids*, Vol. 11, pp. 357-372, 1963.

2. Tsai, S.W. and E.M. Wu, "A General Theory of Strength for Anisotropic Materials," *Journal of Composite Materials*, vol. 5, pp. 58-80, 1971.

3. Hashin, Z., "Failure Criteria for Unidirectional Fiber Composites," *Journal of Applied Mechanics*, vol. 47, pp. 329-334, 1980.

4. Garnich M.R. and A.C. Hansen, "A Multicontinuum Theory for Thermal-Elastic Finite Element Analysis of Composite Materials," *Journal of Composite Materials*, Vol. 31, no.1, pp. 71-86, 1997.

5. Pipes, R.B., and B.W. Cole, "On the Off-Axis Strength Test for Anisotropic Materials," *Journal of Composite Materials*, Vol. 7, pp. 246-256, 1973.

6. Narayanaswami, R., and H.M. Adelman, "Evaluation of the Tensor Polynomial and Hoffman Strength Theories for Composite Materials," *Journal of Composite Materials*, vol.11, pp. 366-377, 1977.

7. Mayes, J.S., "Micromechanics Based Failure Analysis of Composite Structural Laminates", NSWCCD-65-TR-1999/15, Naval Surface Warfare Center, Carderock Division, West Bethesda, MD, 1999.

8. Welsh, J.S., and D.F. Adams, "Development of a True Triaxial Testing Facility for Composite Materials," UW-CMRG-R-99-102, Composite Materials Research Group, University of Wyoming, Laramie, Wyoming, 1999.

Paper B

Composite Laminate Failure Analysis Using Multicontinuum Theory

by

J. Steven Mayes[a†] & Andrew C. Hansen[b]

[a]*Division of Mechanical Engineering, Alfred University, Alfred, NY, 14802, USA*
[b]*Department of Mechanical Engineering, University of Wyoming, Laramie, WY, 82071, USA*

ABSTRACT

Damage in a composite material typically begins at the constituent level and may, in fact, be limited to only one constituent in some situations. An accurate prediction of constituent damage at sampling points throughout a laminate provides a genesis for progressively analyzing failure of a composite structure from start to finish. Multicontinuum Theory is a micromechanics based theory and associated numerical algorithm for extracting, virtually without a time penalty, the stress and strain fields for a composites' constituents during a routine finite element analysis. A constituent stress-based failure criterion is used to construct a nonlinear progressive failure algorithm for investigating the material failure strengths of composite laminates. The proposed failure analysis methodology was used to simulate the nonlinear laminate behavior and progressive damage of selected laminates under both uniaxial and biaxial load conditions up to their ultimate strength. This effort was part of a broader project to compare the predictive capability of current composite failure criteria.

Keywords: multicontinuum, micromechanics, composite materials, failure criterion, constituent.

NOTATION

$\pm$	Indicates the appropriate tensile or compressive value is used depending on the constituent's stress state.
$\{a\}$	Vector relating constituent to composite thermal strains.
$[A]$	Matrix relating constituent to composite mechanical strains.
CTE	Coefficient of thermal expansion.
$[C]$	Composite stiffness matrix.
$[C_\beta]$	Constituent β stiffness matrix ($\beta = f$ (fiber), m (matrix)).
F_i, F_{ij}	Strength parameters (i,j = 1 to 6).
I_i	Composite transversely isotropic stress invariants (i = 1 to 5).
$I_{i\beta}$	Constituent β transversely isotropic stress invariants (i = 1 to 5).
$^{\pm}K_{i\beta}$	Constituent β failure parameter ($\beta = f$ (fiber), m (matrix)); (i = 1, 4).

---

† To whom correspondence should be addressed. Formerly of the Naval Surface Warfare Center, Carderock Division, Structures and Composites Department, West Bethesda, MD, USA

$^{\pm}S_{ij\beta}$ Constituent β strength in the i,j direction ($\beta = f$ (fiber), m (matrix)); (i,j = 1 to 3).

$^{\pm kl}S_{ij\beta}$ Constituent β stress in the i,j direction when stress $^{\pm}S_{kl}$ is applied ($\beta = f$ (fiber), m (matrix)); (i,j = 1 to 3); (k,l = 1 to 3).

V Volume.

$\{\alpha\}$ Composite coefficients of thermal expansion.

$\{\alpha_{ii\beta}\}$ Constituent β coefficients of thermal expansion ($\beta = f$ (fiber), m (matrix)); (i = 1, 2).

$\underset{\sim}{\varepsilon}$ Composite strain tensor.

$\{\varepsilon\}$ Composite total strain tensor in contracted (matrix) notation.

$\underset{\sim}{\varepsilon}_{\beta}$ Constituent β strain tensor ($\beta = f$ (fiber), m (matrix)).

$\{\varepsilon_{\beta}\}$ Constituent β total strain tensor in contracted notation ($\beta = f$ (fiber), m (matrix)).

$\{\varepsilon_o\}$ Composite thermal strain tensor in contracted notation.

$\{\varepsilon_{\beta o}\}$ Constituent β thermal strain tensor in contracted notation ($\beta = f$ (fiber), m (matrix)).

ϕ_{β} Constituent β volume fraction ($\beta = f$ (fiber), m (matrix)).

$\underset{\sim}{\sigma}$ Composite stress tensor.

$\{\sigma\}$ Composite stress tensor in contracted notation.

σ_{ij} Composite stresses referenced to the local lamina (i,j = 1 to 3) or global laminate (i,j = x to z) coordinate system.

$\underset{\sim}{\sigma}_{\beta}$ Constituent β stress tensor ($\beta = f$ (fiber), m (matrix)).

$\{\sigma_{\beta}\}$ Constituent β stress tensor in contracted notation ($\beta = f$ (fiber), m (matrix)).

$\sigma_{ij\beta}$ Constituent β stresses referenced to the local lamina coordinate system ($\beta = f$ (fiber), m (matrix)); (i,j = 1 to 3).

ΔT Difference between current and reference temperatures.

[1] Identity matrix.

1 INTRODUCTION

A majority of failure criteria developed for composite materials to date can be classified as macromechanical because the criteria attempt to predict failure using composite stress-strain data. A key element of macromechanics is the combining of constituent's properties into a homogeneous set of composite lamina properties and possibly combining lamina properties into homogeneous laminate properties.

In contrast, micromechanical failure analyses retain the individual identities of each lamina and its constituents, thereby allowing interaction among them. Composite properties are utilized in micromechanics analyses but failure of each constituent and its contribution to lamina and laminate failure is emphasized. All micromechanical models are predicated on a complete set of material constants for each constituent that are consistent with those of the composite they

form. This consistency is typically synthesized from a finite element or closed form analytical model of the composite microstructure. Examples of micromechanical approaches can be found in Aboudi[1], Pecknold[2], Rahman[3], and Kwon[4]. A review of these approaches can be found in Mayes[5].

2 MULTICONTINUUM THEORY

Multicontinuum Theory (MCT) is a micromechanics based theory and associated numerical algorithm for extracting, virtually without a time penalty, the stress and strain fields for a composites' constituents during a routine finite element analysis. MCT development is presented in detail for linear-elastic and linear-viscoelastic composite behavior in papers by Garnich and Hansen[6,7]. The elasticity theory is summarized here to emphasize concepts important to implementing a constituent based failure analysis. The present theory assumes: (1) linear elastic behavior of the fibers and nonlinear elastic behavior of the matrix, (2) perfect bonding between the fibers and matrix, (3) stress concentrations at fiber boundaries are accounted for only as a contribution to the volume average stress, (4) the effect of fiber distribution on the composite stiffness and strength is accounted for in the finite element modeling of a representative volume of microstructure, and (5) ability to fail one constituent while leaving the other intact results in a piecewise continuous composite stress-strain curve.

MCT begins with a continuum definition of stress at a point. The concept of stress in homogeneous materials, such as steel, is a familiar one to most engineers. Yet, if looked at on a microscale, one sees that the "homogeneous" material is hardly homogeneous. It is obvious that stresses will vary significantly from point to point across different phases and inclusions. The homogenized value used to characterize the stress tensor at a point in a single continuum material is derived by taking a volume average of all stresses in the region as

$$\underset{\sim}{\sigma} = \frac{1}{V}\int_{D} \underset{\sim}{\sigma}\,(\mathrm{x})\,dV \quad , \tag{1}$$

where D is the region representing the continuum point. The concept of a multicontinuum simply extends this concept to reflect coexisting materials within a continuum point. In particular, consider a composite material with two clearly identifiable constituents as shown in Fig. 1[8]. Using equation (1) for each constituent we can write:

$$\underset{\sim}{\sigma}_f = \frac{1}{V_f} \int_{D_f} \underset{\sim}{\sigma}(\mathbf{x})\, dV, \tag{2}$$

and

$$\underset{\sim}{\sigma}_m = \frac{1}{V_m} \int_{D_m} \underset{\sim}{\sigma}(\mathbf{x})\, dV, \tag{3}$$

where

$$D = D_f \bigcup D_m. \tag{4}$$

Combining equations (1-3) leads to

$$\underset{\sim}{\sigma} = \phi_f\, \underset{\sim}{\sigma}_f + \phi_m\, \underset{\sim}{\sigma}_m, \tag{5}$$

where ϕ_f and ϕ_m are the volume fractions of fiber and matrix respectively. Likewise, for strains we have

$$\underset{\sim}{\varepsilon} = \phi_f\, \underset{\sim}{\varepsilon}_f + \phi_m\, \underset{\sim}{\varepsilon}_m. \tag{6}$$

It is important to note the averaging process that results in these equations. That is, we are not concerned with stress and strain variations through individual constituents within D but only with their average values. This is an information compromise that separates structural analysis from micromechanical analysis. Accounting for stress variations throughout every fiber at every material point in even a modest structure is simply not possible or desirable. In contrast, providing constituent average stress and strain fields opens a new and manageable information window on a composite material's response to a load.

Changing from direct tensor to contracted matrix notation, the elastic constitutive laws for the composite and the constituents are given by

$$\{\sigma\} = [C](\{\varepsilon\} - \{\varepsilon_o\}) \ , \tag{7}$$

$$\{\sigma_f\} = [C_f](\{\varepsilon_f\} - \{\varepsilon_{fo}\}) \ , \tag{8}$$

and

$$\{\sigma_m\} = [C_m](\{\varepsilon_m\} - \{\varepsilon_{mo}\}) \ . \tag{9}$$

Combining equations (5-9), constituent fiber and matrix strain fields, $\{\varepsilon_f\}$and $\{\varepsilon_m\}$ respectively, are derived from the composite strain field $\{\varepsilon\}$ using

$$\{\varepsilon_m\} = \left(\phi_m [1] + \phi_f [A]\right)^{-1} (\{\varepsilon\} - \Delta T \{a\}) \ , \tag{10}$$

and

$$\{\varepsilon_f\} = \frac{1}{\phi_f} (\{\varepsilon\} - \phi_m \{\varepsilon_m\}) \ , \tag{11}$$

where

$$[A] = -\frac{\phi_m}{\phi_f} ([C] - [C_f])^{-1} ([C] - [C_m]) \ ,$$

and

$$\{a\} = ([C] - [C_f])^{-1} ([C]\{\alpha\} - \phi_f [C_f]\{\alpha_f\} - \phi_m [C_m]\{\alpha_m\}) \ .$$

An isothermal version of equation (10) appeared in early work by Hill[9]. Typically $[C_f]$, $[C_m]$, $\{\alpha_f\}$, and $\{\alpha_m\}$, are developed from known material properties of the constituents, while $[C]$ and $\{\alpha\}$ of the composite are developed from micromechanical modeling of an assumed fiber-matrix distribution incorporating the constituent material properties. Hence, $[A]$ and $\{a\}$ are known *a priori* to a structural analysis. A major advantage of a MCT analysis is the increased computational efficiency gained by the theory's decoupling of micromechanical modeling from structural analysis.

MCT's ability to calculate accurate constituent stress and strain fields is dependent on constituent elastic constants derived from experimentally determined composite values. Further, MCT's ability to execute realistic failure analysis is dependent on accurate values for constituent strength parameters, also derived from experimentally determined composite values. The link

establishing a relationship between composite (macro) and constituent (micro) elastic constants is a finite element micromechanics model for a continuous fiber unidirectional composite. The finite element micromechanics model used in this research was advanced by Garnich[10] which contains discussion of its development. Only major components of the model will be summarized here.

The micromechanics model is based on an assumption of uniform hexagonal fiber packing within the lamina's matrix (Fig. 2). A unit cell, representative of the repeating microstructure, is extracted from a region bounded by symmetry lines. Unit cell geometry, fiber volume fraction, and boundary conditions are used to define the finite element model (Fig. 3). The unit cell is based on a generalized plane strain assumption in the fiber direction but is fully three-dimensional. The cell is modeled with a finite element scripting language allowing material properties and fiber volume fraction to be varied as required. Boundary conditions[10,11] necessary to enforce compatibility of unit cell boundaries with adjacent unit cells are generated automatically. Four linear elastic load cases are solved (longitudinal tension, transverse tension, transverse shear, and longitudinal shear) to determine and verify five independent elastic constants for transversely isotropic composite lamina.

All constituent elastic constants (Tables 1-2) and strengths (Tables 3-4) were backed out via the micromechanics model from experimentally determined composite values provided by the organizers[12]. These *in situ* constituent values used in the MCT analyses conducted herein were different than those presented for this exercise by the organizers.

3 FAILURE CRITERION

The Maximum Distortional Energy, or von Mises, criterion is the most widely used criterion for predicting yield points in isotropic metals[13]. The isotropic von Mises failure criterion is a special case of a general form of quadratic interaction criteria, so named because they include

terms to account for interaction between the stress components. Variations of the general criteria have been used to predict brittle failure in orthotropic materials[14].

A generalized quadratic interaction failure criterion, suggested by Gol'denblat and Kopnov[15] and proposed by Tsai and Wu[16], is given as

$$F_i\sigma_i + F_{ij}\sigma_i\sigma_j = 1, \tag{12}$$

where F_i and F_{ij} are experimentally determined strength tensors and contracted tensor notation is used (i,j = 1 to 6). Hoffman[17] has suggested that the linear terms, F_i, are necessary to account for differences in tensile and compressive strengths whereas Tsai and Wu state that they are necessary to account for internal stresses. Tsai and Wu[16] presented a form of equation (12) for transversely isotropic composites as

$$\begin{aligned} F_1\sigma_{11} + F_2(\sigma_{22}+\sigma_{33}) + F_{11}\sigma_{11}^2 + F_{22}(\sigma_{22}^2+\sigma_{33}^2+2\sigma_{23}^2) + F_{66}(\sigma_{12}^2+\sigma_{13}^2) \\ + 2F_{12}(\sigma_{11}\sigma_{22}+\sigma_{11}\sigma_{33}) + 2F_{23}(\sigma_{22}\sigma_{33}-\sigma_{23}^2) = 1. \end{aligned} \tag{13}$$

Hashin[18] developed a three-dimensional, stress interactive, failure criterion for unidirectional lamina that recognized two distinct and uncoupled failure modes. While the failure criterion itself was based on composite stresses, it constructs a piecewise continuous failure form based on constituent failure modes. The failure criterion assumes transverse isotropy for a unidirectional composite. A local orthogonal coordinate system is defined in which the fiber axis serves as the principal, x_1, material direction, and x_2, x_3 the transverse and through-thickness directions. The failure state of the material is expressed in terms of transversely isotropic stress invariants. Although Hashin derived these invariants, Hansen[19], in development of an anisotropic flow rule for plastic behavior in composite materials, presented a different form used within this paper. The five transversely isotropic stress invariants are:

$$
\begin{aligned}
I_1 &= \sigma_{11}, \\
I_2 &= \sigma_{22} + \sigma_{33}, \\
I_3 &= \sigma_{22}^2 + \sigma_{33}^2 + 2\sigma_{23}^2, \\
I_4 &= \sigma_{12}^2 + \sigma_{13}^2, \\
I_5 &= \sigma_{22}\sigma_{12}^2 + \sigma_{33}\sigma_{13}^2 + 2\sigma_{12}\sigma_{13}\sigma_{23}.
\end{aligned} \tag{14}
$$

Hashin's choice of a quadratic form eliminates I_5 from appearing in the failure criterion. Therefore the most general form for a quadratic criterion[18] is

$$K_1 I_1 + L_1 I_1^2 + K_2 I_2 + L_2 I_2^2 + M_{12} I_1 I_2 + K_3 I_3 + K_4 I_4 = 1 \ , \tag{15}$$

where K_i, L_i, and M_{12} are experimentally determined failure coefficients.

At this point, it is instructive to compare the criterion of Tsai and Wu with that of Hashin. Rewriting equation (13) in terms of the transversely isotropic stress invariants gives

$$F_1 I_1 + F_2 I_2 + F_{11} I_1^2 + F_{22} I_3 + F_{66} I_4 + 2F_{12} I_1 I_2 + 2F_{23}\left(I_2^2 - I_3\right) = 1,$$

or rearranging,

$$F_1 I_1 + F_{11} I_1^2 + F_2 I_2 + 2F_{23} I_2^2 + 2F_{12} I_1 I_2 + \left(F_{22} - 2F_{23}\right) I_3 + F_{66} I_4 = 1. \tag{16}$$

Comparing equation (16) to equation (15), shows that the Tsai-Wu criterion for transversely isotropic materials and the Hashin failure criterion have the same functional form. Their difference is in defining the coefficients of the stress terms. The Tsai-Wu equation is used to define a smooth and continuous failure surface in both the tension and compression regions of space. As a result the coefficients are functions of both tensile and compressive composite strengths. In contrast, Hashin identified two composite failure modes; fiber versus matrix influenced, and developed separate equations based on the failure mode to determine a failure state. Hashin further recognized that a composite typically has different ultimate strengths in tension and compression, so both fiber and matrix failure criteria have tensile and compressive subforms. Hence the coefficients of the stress terms are functions of only tension or compression strengths resulting in a piecewise continuous stress-space failure surface.

In what follows, we adopt the view of Hashin and develop separate failure criteria for the fiber and matrix failure modes. However, in a major departure from Hashin's work, we develop failure criteria in the form of equation (15) for *each constituent* as opposed to the composite by utilizing constituent stress information produced by MCT. As a consequence, the transversely isotropic stress invariants, defined in equation (14), were used for each constituent of the composite material under consideration. Furthermore, recognizing that constituents typically have different ultimate strengths in tension and compression, each constituent failure criterion has a tensile and compressive subform.

A unique aspect of the MCT failure theory is that an anisotropic failure theory is used on an isotropic matrix material. This complexity is necessitated by the fact that the matrix failure behavior will be anisotropic due to microstructural geometry. The root of this phenomenon can be conceptualized by considering a transversely isotropic unidirectional composite. If all fibers were removed but their holes retained only a matrix of "Swiss Cheese" would remain. Because of the remaining microstructure, macroscopic failure of the material will be fundamentally different in axial versus transverse directions resulting in a transversely isotropic failure envelope.

As a first approximation, we would like to simplify equation (15) for each of the constituents. Pipes and Cole[20] demonstrated some of the difficulties in experimentally determining stress interaction terms such as M_{12}, analogous to F_{12} in the Tsai-Wu theory. Further, Narayanaswami[21] demonstrated numerically that setting the stress interaction term F_{12} to zero in the Tsai-Wu quadratic failure criterion in plane stress analyses resulted in less than 10% error for all the load cases and materials considered. Hence, we set M_{12} equal to zero. Tsai and Wu identify the linear terms in equation (13) as necessary to account for internal stresses. Internal stresses refer to self equilibrating stresses within each constituent which, when added together according to equation (5), produce no composite stress. Internal stresses may arise in composites operating at a temperature other than the reference temperature due to a mismatch in constituent coefficients of thermal expansion. These internal stresses are accounted for in the formulation of

Multicontinuum Theory through the $\{a\}$ vector. Thus we eliminate the linear terms from equation (15). If analytical comparisons against experimental results do not provide a satisfactory correlation, these terms, along with the term M_{12}, could be reexamined for their potential contributions.

Noting the above, the general form for a stress interactive failure criterion, after changing to a consistent coefficient notation, is given by

$$K_1 I_1^2 + K_2 I_2^2 + K_3 I_3 + K_4 I_4 = 1. \tag{17}$$

Developing a form of equation (17) for fiber failure we note that the majority of fibers used for composite reinforcement have greater transverse strengths than the matrices commonly used in conjunction with them. Hence, we assume that transverse failure of these composites is matrix dominated. Based on this assumption, we set K_2 and K_3 equal to zero in equation (17) as their associated stress invariants involve transverse normal stresses. The fiber failure criterion reduces to

$$K_{1f} I_{1f}^2 + K_{4f} I_{4f} = 1. \tag{18}$$

To determine coefficients for each stress term, we solve equation (18) considering individual load cases of pure in-plane shear, tension, and compression applied to unidirectional lamina. For the case of in-plane shear load only ($\sigma_{12f} \neq 0$, $\sigma_{11f} = 0$), we find

$$K_{4f} = \frac{1}{S_{12f}^2},$$

where, S_{12f} denotes fiber shear strength. For the case of tensile load only ($\sigma_{11f} > 0$; $\sigma_{12f} = 0$), we find

$$^{+}K_{1f} = \frac{1}{{}^{+}S_{11f}^2}.$$

For the case of compression load only ($\sigma_{11f} < 0$; $\sigma_{12f} = 0$), we find

$$^{-}K_{1f} = \frac{1}{^{-}S_{11f}^2}.$$

The criterion for fiber failure can now be expressed as

$$^{\pm}K_{1f}I_{1f}^2 + K_{4f}I_{4f} = 1. \tag{19}$$

The ± symbol indicates that the appropriate tensile or compressive ultimate strength value is used depending on the constituent's stress state.

To determine the coefficients of equation (17) for matrix failure we first solve the equation considering load cases of pure in-plane and transverse shear. For the case of transverse shear only ($\sigma_{23m} \neq 0$, $\sigma_{11m} = \sigma_{22m} = \sigma_{33m} = \sigma_{12m} = 0$), we find

$$K_{3m} = \frac{1}{2S_{23m}^2}.$$

For the case of in-plane shear only ($\sigma_{12m} \neq 0$, $\sigma_{11m} = \sigma_{22m} = \sigma_{33m} = \sigma_{23m} = 0$), we find

$$K_{4m} = \frac{1}{S_{12m}^2}.$$

Noting that a majority of fibers used for composite reinforcement have greater longitudinal strengths than the matrices commonly used in conjunction with them, we assume that the longitudinal failure of these composites is fiber dominated. Based on this assumption and some numerical sensitivity studies we set K_{1m} equal to zero. The approach to our 'sensitivity analysis' was to conduct failure analyses, with and without parameter K_{1m} in the proposed failure criteria, on all available test cases. We determined that the presence of K_{1m} did not significantly affect failure predictions results for those cases. Incorporating these results into (17) gives

$$K_{2m}I_{2m}^2 + \frac{1}{2S_{23m}^2}I_{3m} + \frac{1}{S_{12m}^2}I_{4m} = 1. \tag{20}$$

To determine K_{2m}, we consider the case of transverse tensile load only ($(\sigma_{22m} + \sigma_{33m}) > 0$, $\sigma_{23m} = \sigma_{12m} = 0$) and find

$$^{+}K_{2m} = \frac{1}{\left(^{+}S_{22m} + ^{+22}S_{33m}\right)^2}\left(1 - \frac{^{+}S_{22m}^2 + ^{+22}S_{33m}^2}{2S_{23m}^2}\right).$$

The numeric superscripts ("22") in the above failure parameters are used to denote the direction of the applied load. Note that while a pure transverse (one-dimensional) load, σ_{22}, on a composite lamina results in

$$\sigma_{11} = \sigma_{33} = 0,$$

the constituents experience a fully three-dimensional stress state[6,7]. Likewise, for the case of a pure transverse compressive load ($(\sigma_{22m} + \sigma_{33m}) < 0$, $\sigma_{23m} = \sigma_{12m} = 0$)

$$^{-}K_{2m} = \frac{1}{\left(^{-}S_{22m} + ^{-22}S_{33m}\right)^2}\left(1 - \frac{^{-}S_{22m}^2 + ^{-22}S_{33m}^2}{2S_{23m}^2}\right).$$

The criterion for matrix failure can now be expressed as

$$^{\pm}K_{2m} I_{2m}^2 + K_{3m} I_{3m} + K_{4m} I_{4m} = 1. \tag{21}$$

Transverse shear strength values were not provided as part of the material characterizations provided by the organizers[12]. Parameter $^{\pm}K_{2m}$ is highly sensitive to these values and rather than risk using inaccurate values, the matrix failure criterion was modified. Expanding equation (21) in terms of local stress components gives

$$^{\pm}K_{2m}\left(\sigma_{22m} + \sigma_{33m}\right)^2 + K_{3m}\left(\sigma_{22m}^2 + \sigma_{33m}^2 + 2\sigma_{23m}^2\right) + K_{4m}\left(\sigma_{12m}^2 + \sigma_{13m}^2\right) = 1.$$

For the load cases considered in this paper, no transverse shear stresses arise in the constituents so we set $\sigma_{23m} = 0$ and rearrange the above as

$$(^{\pm}K_{2m} + K_{3m})\sigma_{22m}^2 + (^{\pm}K_{2m} + K_{3m})\sigma_{33m}^2 + ^{\pm}K_{2m}\left(2\sigma_{22m}\sigma_{33m}\right) + K_{4m}\left(\sigma_{m12}^2 + \sigma_{13m}^2\right) = 1. \tag{22}$$

$^{\pm}K_{2m}$ scales a stress interaction in the third term of equation (22). We set this scale factor to zero as was done previously in the simplification of equation (15). This results in

$$^{\pm}K_{3m}(\sigma_{22m}^2 + \sigma_{33m}^2) + K_{4m}\left(\sigma_{12m}^2 + \sigma_{13m}^2\right) = 1.$$

Therefore, in terms of the transversely isotropic stress invariants, the modified matrix failure criterion becomes

$$^{\pm}K_{3m}I_{3m} + K_{4m}I_{4m} = 1, \tag{23}$$

where

$$^{\pm}K_{3m} = \frac{1}{^{\pm}S_{22m}^2 + ^{\pm 22}S_{33m}^2}.$$

The mode of failure, fiber or matrix, is determined by monitoring their failure criteria given by equations (19) and (23), respectively. The relative contribution of the various stress components to initial, intermediate, and final failure states can be determined by examining the product of the failure parameter $K_{i\beta}$ and its associated stress invariant $I_{i\beta}$ (For examples, see Table 6 through Table 13).

4 DESCRIPTION OF ANALYSIS METHOD

A numerical MCT algorithm, based on equations (10) and (11), was developed and incorporated into an in-house finite element code[22]. While the finite element approach may be more powerful than necessary for the analyses conducted as part of this exercise, the methodology was originally developed for failure analyses of general composite structures. Using the finite element framework provides a high degree of analytical flexibility.

A majority of composite materials in use today have organic matrices that produce significant nonlinear shear stress-strain behavior as demonstrated by the shear stress-strain curves presented by the organizers[12]. For the research considered herein, unloading or sustained creep of the composite was not a consideration. Therefore, a nonlinear-elastic constitutive model, as developed by Mayes[22], relating changes in elastic constants due to changing composite shear modulus was used. The model uses a three-term exponential series of the form

$$\tau = B_0 + B_1 e^{(h_1\gamma)} + B_2 e^{(h_2\gamma)}, \tag{24}$$

to fit in-plane experimentally determined composite shear stress-strain curves. B_i and h_i are curve fit parameters, τ is shear stress (Pa), and γ is engineering shear strain (dimensionless). Nonlinear regression was used to fit the five equation parameters to experimental shear data (Table 5). A strain dependent, tangent shear modulus was computed from the first derivative of equation (24) for use during a finite element analysis. Tension and compression elastic moduli for all lamina were assumed to be constant.

In the finite element method, numerical integration samples stress, strain, and material values at Gauss quadrature points. MCT failure analyses store a state variable corresponding to composite material damage for every Gauss point. Three composite material conditions or states, listed in increasing damage severity, are defined as:

1. Undamaged composite,
2. Composite damaged by matrix failure, and
3. Composite damaged by fiber failure.

When either constituent fails, all its moduli are immediately reduced to a near zero value at that Gauss point. Near zero values are used rather than zero to avoid numerical difficulties. Matrix moduli are reduced to 1% of their original value. Fiber moduli, which are typically one to two orders of magnitude larger than matrix moduli, are reduced by whatever percentage is required to bring damaged fiber values to the same magnitude as damaged matrix so that near zero stiffness values are the same for both constituents. Poisson's ratios remain constant. Their values are rendered irrelevant by the use of near zero moduli values which scale elements of the stiffness matrix, $[C_\beta]$, to near zero values. Since all constituent properties, both intact and failed, are known *a priori,* the micromechanics model (Fig. 3) is used to determine two additional sets of composite properties, corresponding to damage states 2 and 3, before conducting a MCT failure analysis.

The nonlinear character of a failure analysis requires the load to be incrementally applied and the damage tracked progressively. Initially, composite material properties are set to an

undamaged condition. At each load step a damage algorithm, using the failure criteria formulated in equations (19) and (23), checks every Gauss point for constituent failure based on cumulative stresses. When constituent failure is detected at a Gauss point, stresses are recalculated using accumulated strains and updated material properties. Gradual softening of the structure due to composite damage at the Gauss points and a nonlinear-elastic constitutive model causes an equilibrium imbalance between the applied (external) and resisting (internal) load vectors. A standard Modified Newton-Raphson nonlinear iterative procedure within each load step calculates differences between external and internal load vectors and applies it to the structure as a "virtual" load. The net effect is to increase nodal displacements, hence Gauss point strains and stresses, until equilibrium is restored and the next load step is then applied.

Structural failure of a laminate is defined as that point in the load history when the structure can no longer support the accumulated load and deflections begin to grow without bound. Unbounded growth is detected during equilibrium iterations by monitoring changes in the Euclidean (L_2) norm of the structural displacement vector.

5 MCT SIMULATIONS OF LOAD-RESPONSE TO FAILURE FOR SELECTED LAMINATES

Unidirectional (UD) E-glass/LY556/HT907/DY063 and T300/BSL914C lamina failure envelopes under biaxial normal-shear loads are shown in Fig. 4 and Fig. 5. These failure envelopes were symmetric about the abscissa and showed a typical quadratic shape caused by interactions between normal and shear stresses in the failure criteria. The weaker matrix was the primary load carrying constituent in the σ_y-τ_{xy} loading of the unidirectional (UD) E-glass/LY556/HT907/DY063 lamina. Thus matrix failure determined the final failure envelope. In contrast, the stronger fiber was the primary load carrying constituent in the σ_x-τ_{xy} biaxial loading of the T300/BSL914C lamina. As a result the lamina failure envelope is sharply skewed in the σ_x direction. The failure envelope for a UD E-glass/MY750 lamina under biaxial σ_x/σ_y

load is presented in Fig. 6. This envelope was characterized by a distinct transition from fiber to matrix failure resulting in a shape analogous to one that would be produced by a simple maximum stress failure criterion ($^{\pm}\sigma_{ijf}/^{\pm}S_{ijf}$ or $^{\pm}\sigma_{ijm}/^{\pm}S_{ijm}$). Initial and final lamina failure envelopes in Fig. 4 through Fig. 6 were identical.

Initial and final failure envelopes for an E-glass/LY556/HT907/DY063 $[90°/\pm30°]_S$ laminate under biaxial σ_y/σ_x load are shown in Fig. 7. The final failure envelope exhibits a complex shape because of stress interactions between lamina and changing failure modes between constituents. Results for the initial and final failure envelopes are summarized in Table 6 and Table 7.

The horizontal edge of the initial failure envelope, points a to b, was caused by matrix tensile failure in the ±30° lamina. The right edge of the initial failure envelope between points b to c is due to matrix tensile failure 90° lamina. Intermediate damage, in the form of matrix failure, occurred later in the ±30° lamina due to combined tensile and shear stresses. Note that in this regime, all matrix in the laminate had failed but the laminate continued to sustain load. Between points c and d, initial matrix damage slowly switches to a combined compression and shear failure in the ±30° lamina. From points d to e, the initial and final failure envelopes coincided with compressive matrix failure in the ±30° lamina controlling the mode. Initial failure from points e to a was due to matrix compressive failure in the 90° lamina.

Along the upper edge of the final failure envelope from points A to B, failure began with combined fiber compression-shear failure in the ±30° lamina and shifted to fiber tensile failure in the 90° lamina. Catastrophic laminate failure occurred between points B and C due to combined fiber tensile-shear failure in the ±30° lamina. Fibers in the 90° lamina were still intact. A change in the failure envelope shape occurred between points C and D where the failure mode switched to *compressive* fiber failure in the 90° lamina (in the *tension-tension* quadrant I) leaving fibers in the ±30° lamina intact. Between points D and E, simultaneous fiber failure occurred in the 90°

(compressive) and ±30° (shear) lamina. From points E to F, catastrophic laminate failure became increasingly dependent on fiber shear failure in the ±30° lamina. From points F to G, the initial and final failure envelopes coincided with compressive matrix failure in the ±30° lamina which precipitated fiber compressive failure in the 90° lamina. The mechanism for final failure shifted to fiber shear in the in the 30° lamina for the points G to H.

Initial and final failure envelopes for an E-glass/LY55/HT907/DY063, $[90°/\pm30°]_s$ laminate under biaxial, σ_x/τ_{xy}, load are shown in Fig. 8. The failure envelope was symmetric about the σ_x axis. Results for both failure envelopes are summarized in

Table 8 and Table 9.

Initial laminate damage in quadrant II, between points a and b, was due to compressive matrix failure in the 90° lamina. Initial failure between points b and c began with combined compression/shear matrix failure in the 90° lamina and tensile/shear matrix failure in the -30° lamina. The failure mode shifted to matrix tension closer to point c. Between points c and d, initial failure was due to tensile matrix failure in the 90° lamina.

The step-like shape of the final failure envelope between points A to B was caused by fiber failure oscillating between the ±30° lamina under combined compressive and shear stresses. In the region about point B, the initial and final failure envelopes coincided. Simultaneous matrix failure in the 90° (compressive) and -30° (tensile) lamina precipitated fiber failure in both the -30° and +30° lamina. From point C to D, the final failure mode transitioned from fiber compressive failure at C to fiber tensile fiber failure at D in the -30° lamina. At point E, the final failure mode switched to tensile fiber failure in the +30° lamina but became increasingly dependent on the shear contribution as one moved towards point F. At point G, final failure began as matrix failure in the -30° lamina, due to combined tensile and shear stresses, which precipitated fiber shear failure in the +30° lamina. A shape change in the failure envelope

occurred at point H due to a switch in failure mode to simultaneous fiber failure in the +30° lamina (tensile and shear) and 90° lamina (tensile).

Both initial and final failure envelopes for a AS4/3501-6, $[0°/\pm45°/90°]_S$ laminate under biaxial, σ_y/σ_x, load are shown in Fig. 9. The failure envelope was symmetric about a line through points A and H. Results for the failure envelopes are summarized in

Table 10 and Table 11.

The initial failure envelope between points a and c was defined by matrix tensile failure in the 90° lamina. At point a, simultaneous matrix failure occurred in all lamina but the laminate retained the ability to sustain load. Later in the load history intermediate laminate damage, in the form of matrix failure in the ±45° lamina, occurred to the right of points b to c due to combined tensile and shear stresses. The initial and final failure envelopes coincided at point c. Failure there was due initially to matrix failure in the 90° (tension) and ±45 (shear) lamina precipitating compressive fiber failure in the 90° lamina.

Final failure between points A and B was due to fiber tensile failure in the 0° lamina. An abrupt change in shape of the failure envelope occurred at point B as the failure mode shifted to fiber shear stress in the ±45 lamina. Between points C and D tensile fiber failure in the 0° lamina and compressive fiber failure in the 90° lamina determined final laminate failure. Fiber shear stresses precipitated failure in the ±45° lamina between points D and E. From points F to H final failure was determined by compressive failure of the fiber in the 90° lamina.

The stress-strain curves for a AS4/3501-6, $[0°/\pm45°/90°]_S$ laminate under uniaxial tension $\sigma_y/\sigma_x = 1/0$ and $\sigma_y/\sigma_x = 2/1$ are shown in Fig. 10 and Fig. 11, respectively. Strain jumps in both plots indicate that initial laminate damage occurred due to transverse matrix tensile failures in the 0° lamina. Intermediate damage in the form of matrix failure in the ±45° lamina was caused by combined shear and tensile stresses. Under the $\sigma_y/\sigma_x = 2/1$ load, additional intermediate damage

occurred through tensile matrix failure in the 90° lamina. Final failure in both laminates was caused by tensile fiber failure in the 90° lamina.

The E-glass/MY750/HY917/DY063 failure envelope for a $[\pm 55°]_S$ laminate under biaxial, σ_y / σ_x, load is shown in Fig. 12. Initial and final failure envelopes were identical. Results for the failure envelope are summarized in Table 12.

Tensile matrix failure in all lamina determined failure from points A to B. It is interesting to note that the E-glass/LY55/HT907/DY063, $[90°/\pm 30°]_S$ and the AS4/3501-6, $[0°/\pm 45°/90°]_S$ laminates under σ_y / σ_x loading also experienced complete matrix failure in quadrant I but continued to load. From points B to D, rising shear stresses combined with tensile stresses to cause matrix failure. The rough envelope edge around point C was due to the manner in which the load was applied, i.e., load step size and σ_y / σ_x ratio, and does not have physical significance. From points D to E fiber failure under combined shear and compressive stress caused laminate failure. Matrix failure due primarily to compressive stresses determined the failure envelope from points E to F. Rising shear stresses combined with the compressive stresses caused matrix failure between points F and G. Failure due to fiber shear stress began at point G and slowly shifted to fiber tensile failure at point H.

Non-linear shear behavior characterized the stress-strain curves of the E-glass/MY750/HY917/DY063, $[\pm 55°]_S$ laminate under uniaxial load, $\sigma_y / \sigma_x = 1/0$, as shown in Fig. 13. Catastrophic laminate failure was caused principally by shear failure of the fibers. Non-linear shear effects did not become significant for the $[\pm 55°]_S$ laminate under biaxial loading, $\sigma_y / \sigma_x = 2/1$, (Fig. 14) because catastrophic matrix tensile failure occurred at relatively low strain levels.

The E-glass/MY750/HY917/DY063 stress strain curves for a [0°/90°/0] laminate under uniaxial load $\sigma_y/\sigma_x = 1/0$ are shown in Fig. 15. Initial laminate damage due to tensile matrix failure in the 0° lamina occurred at approximately one-third of the ultimate laminate load. This

damage is a consequence of the load being applied transversely to the fiber direction in the 0° lamina. Intermediate laminate damage, which was also in the form of matrix tensile failure, occurred in the 90° lamina. This matrix damage was interesting because it occurred in the principal load bearing (σ_{11f}) direction which was aligned with the load. Note that there is no term in the matrix failure criterion, equation (23), involving stress σ_{11m}. Therefore this matrix failure was caused by transverse, σ_{22m} and σ_{33m}, stresses arising from Poisson's effect. Tensile fiber failure in the 90° lamina resulted in final laminate failure.

Stress-strain curves for a E-glass/MY750/HY917/DY063, $[\pm 45°]_S$ laminate exhibited near linear response under σ_y/σ_x = 1/1 biaxial load as shown in Fig. 16. Catastrophic tensile failure of the matrix occurred before any significant lamina shear stresses developed. In contrast, Fig. 17 shows a highly nonlinear stress-strain response in a $[\pm 45°]_S$ laminate under σ_y/σ_x = 1/-1 biaxial load. These shear induced, laminate strains did not become significantly nonlinear until about the 0.5% level which was approximately twice the ultimate laminate strain in the previous σ_y/σ_x = 1/1 load case. Laminate failure under biaxial load σ_y/σ_x = 1/-1 is due to fiber shear failure.

6 COMMENTS ON THE MCT FAILURE RESULTS

The failure load (stress) for individual points on a failure envelope was taken as the value at the beginning of the load step in which failure occurred. The failure value is therefore dependent on the size of the load step but will monotonically converge with decreasing load step size. Generally the lack of smooth failure envelope edges, (e.g., Fig. 8 in the II and III quadrants) is a result of discrete loading ratios and load step size and has no physical significance. Generating a single 2-dimensional failure envelope took on the order of a hundred finite element runs so time constraints prevented detailed convergence of the failure surfaces. Other rough edges, e.g. Fig. 8 on the positive σ_x axis, are due to changes in failure modes from matrix to fiber and may have physical significance.

Establishing initial, intermediate, and final failure envelopes serves to highlight the importance of assessing constituent damage in a structural analysis. The practical implications of the different failure surfaces are in establishing allowable stress levels in a composite design, .e.g., at what degree of laminate damage is composite 'failure' deemed to have occurred?

The MCT approach to failure analysis requires identifying constituent failure modes from composite test data. Identifying the constituent that precipitates failure in longitudinal and transverse lamina tension and compression tests is intuitive and straightforward, i.e., fiber failure for longitudinal loads and matrix failure for transverse loads. Identifying the constituent leading to shear failure is more problematic, as non-catastrophic matrix and fiber damage begins well before ultimate composite strength is achieved[23]. Ultimate constituent shear strengths have previously been determined by utilizing nonlinear regression analysis of load cases involving varying amounts of combined normal and shear stresses[5]. Specifically, we make an educated guess as to each constituents shear strength and then use that data to predict lamina failure in off-axis tension tests. Using the experimentally determined lamina failures and our initial guess, we iterate with additional guesses until failure predictions based on constituent shear failure produce composite failures that more or less agree with the experimental data. Armed with these semi-empirical constituent shear strengths we have increased confidence in analysis of more complex problems involving shear.

Data from off-angle, balanced, symmetric laminates, $[\pm\theta]_S$, provide an excellent basis for determining a best fit determination of failure parameters S_{12m} , S_{23m} , and S_{12f}. Hence, some of the laminates analyzed as part of this exercise would, in a normal case, be used as inputs to the failure prediction process.

Thermal effects due to curing were neglected in all analyses conducted as part of the failure exercise. However, as noted previously, *in situ* material properties, as determined from finite element micromechanics, were utilized in this failure analysis. Differences between the *in situ* properties used herein and those provided by the organizers may be explained in part by

residual thermal stresses. MCT can account for post-cure thermal effects through the thermal vector, {a}, in equation (10).

MCT's handling of thermal effects can be demonstrated using the E-glass/MY750/HT917/DY063 composite as an example. The organizers provide a stress-free reference temperature of 120 °C for this material. We assume that uniaxial testing used to determine lamina composite tensile strengths occurred at 20 °C. Conducting an MCT analysis of the uniaxial strength test, with a ΔT = -100 °C, we backed out the temperature adjusted normal constituent tensile strengths shown in

Table 13. A negative ΔT produces internal matrix tensile stresses. Accounting for this internal tensile load has the net effect of increasing matrix tensile strength and reducing matrix compressive strength. A ΔT= -100°C has no significant effect on the E-glass fiber normal strengths. Next we reanalyzed test case numbers 12 and 13, i.e., σ_y/σ_x = 1/0 loading of the $[\pm 45°]_S$ and the [0°/90°/0°] laminates, again assuming a ΔT = -100°C. The MCT program applies ΔT in its entirety as a uniform temperature in the first load step.

In the thermal analysis of the [0°/90°/0°] laminate, shown in Figure 19, applying a ΔT = -100°C in the first load step initially caused both laminate strains, ε_x and ε_y, to be negative. As the y-direction mechanical load increases, the total strain in that direction becomes positive. We note that by defining the strain to be zero under a composite stress-free state, and after the thermal load has been applied, the initial jump into negative strain territory would not appear.

The presence of residual stresses in the thermo-mechanical analysis have an interesting effect on the matrix failures occurring during the loading program. Specifically, the residual stresses lead to a decrease in the initial failure stresses and an increase in the intermediate failure stresses when compared to the pure mechanical analysis. This phenomenon is attributed to two competing effects of the residual stresses.

To begin, we emphasize that matrix failures in this load case are due to stresses transverse to the fiber. Furthermore, Table 13 shows the residual stresses have the effect of increasing the temperature adjusted transverse tensile strengths. Countering the effect of increased matrix transverse strengths is the presence of large residual stresses due to the thermal load (See Table 14). Focusing on σ_{22m} in Table 14, the residual matrix stress varies due to the constraining influence of adjacent lamina and, in fact, is significantly larger in a $0^{\circ}/90^{\circ}$ laminate as compared to a unidirectional laminate. The increase in residual stress in the $0^{\circ}/90^{\circ}$ configuration more than offsets the increased transverse tensile strengths in the residual stress analysis. The net effect is that failure occurs earlier in the thermo-mechanical problem as seen in Figure 18.

The MCT analysis of the thermo-mechanical problem also shows that initial matrix failure in the 0° lamina produces significant matrix stress relief in the 90° lamina. The stress relief is sufficient such that the increased matrix strengths in the thermo-mechanical analysis dominate any remaining residual stress effects. The result is an increase in the predicted intermediate failure stress when compared to the purely mechanical analysis.

The data listed in Table 15 show that the ultimate strength of the $[\pm 45^{\circ}]_S$ laminate under uniaxial load is significantly reduced due to the combination of thermal and mechanical induced matrix tensile stresses. As in the case of the $[0^{\circ}/90^{\circ}]_S$ laminate, the orthogonal orientation of the $\pm 45^{\circ}$ lamina fibers restrains the matrix thermal contraction inducing high matrix tensile stresses. Strength of the $[\pm 45^{\circ}]_S$ laminate under biaxial, $\sigma_y/\sigma_x = 1/1$, loading, shown in Fig. 19, is also significantly lowered in the presence of a thermal load $\Delta T = -100^{\circ}C$. Even though composite strains in the x and y directions are negative throughout the load history, the laminate fails due to matrix tensile stresses.

Clearly the exercise above indicates that thermally induced residual cure stresses can be important. But the absence of a precise thermo-mechanical constitutive law describing the

complex interactions between the fiber and the liquid-to-solid transition of the matrix occurring at high curing temperatures, makes accounting for stresses induced during the cure process a questionable endeavor.

7 CONCLUDING REMARKS

MCT is a fully 3-dimensional failure prediction methodology intended to efficiently bring constituent information to bear on the analysis of general composite structures. Because failure of composite laminates begins at the constituent level, the constituent information provided by MCT has tremendous value. Accurate predictions of constituent level failure, within the framework of the finite element method, enables development of a progressive failure analysis for general structures. Permitting only one constituent to fail while keeping the others intact allows load redistribution to other parts of the structure as well as to the remaining constituents. Material failure can be tracked as it occurs region by region. The stiffness and strength of damaged areas can be reduced without necessarily declaring total structural failure. This approach has not been incorporated in general design practice in the past because constituent information was generally unavailable in standard finite element analysis.

8 ACKNOWLEDGEMENTS

The research reported herein was supported by the In-house Laboratory, Independent Research program at the Naval Surface Warfare Center, Carderock Division and by the Office of Naval Research under Grant N00014-97-1-1081.

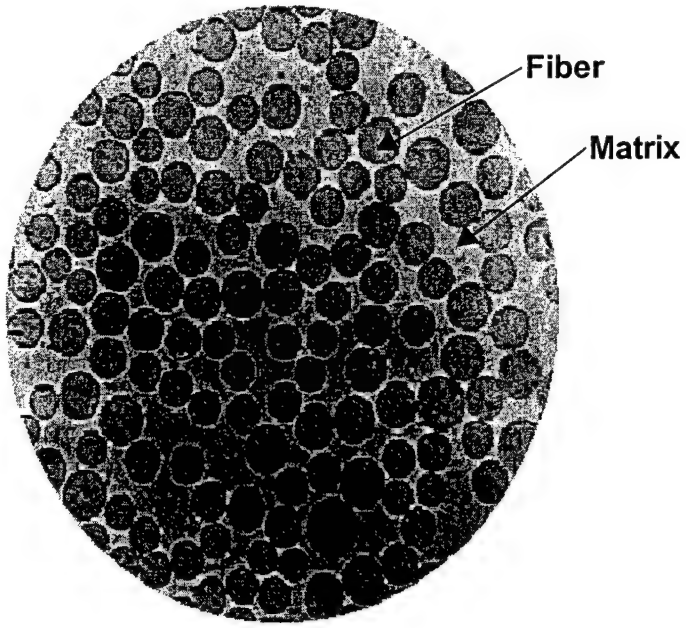

Fig. 1 *Composite lamina as a multicontinuum.*

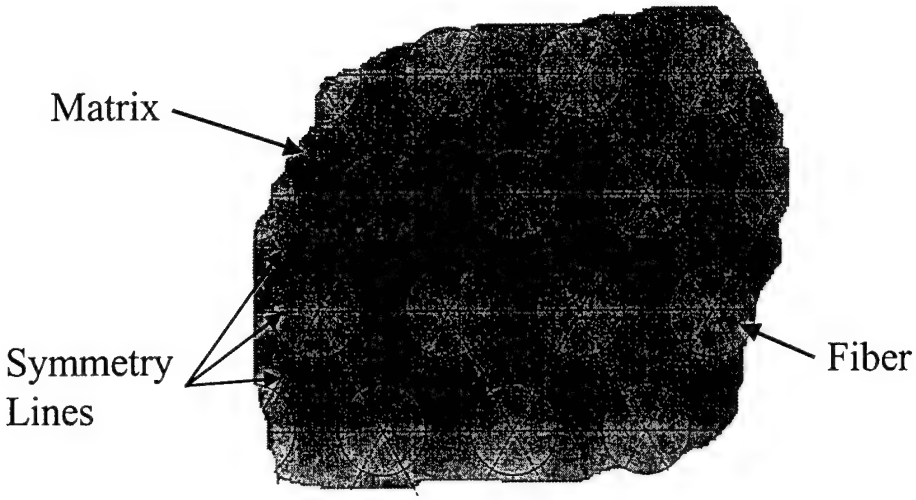

Fig. 2 *Idealized lamina microstructure.*

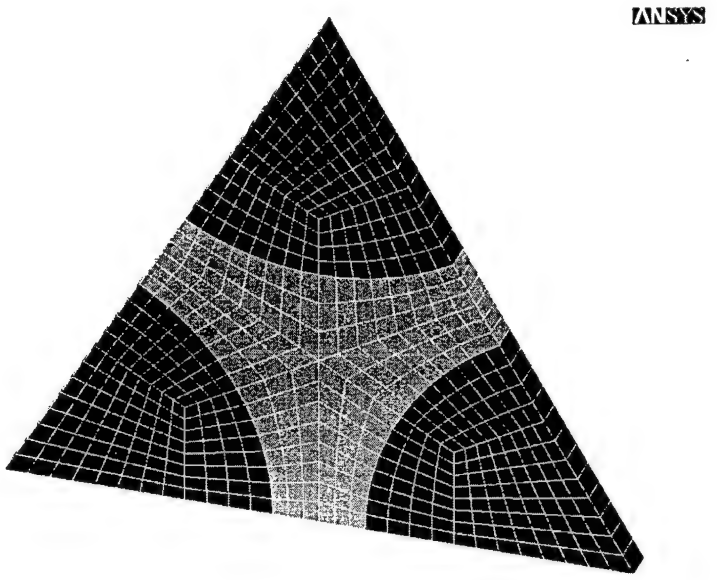

Fig. 3 *Finite element model of a unit cell created using the ANSYS software.*

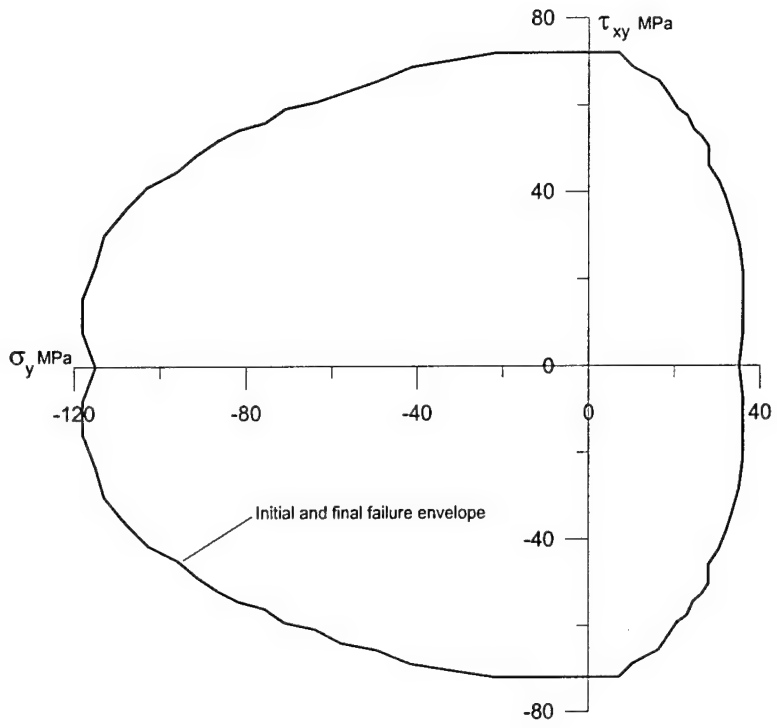

Fig. 4 *Failure envelope for a [0°] lamina made from E-glass/LY556/HT907/DY063 under biaxial, σ_y/τ_{xy}, load.*

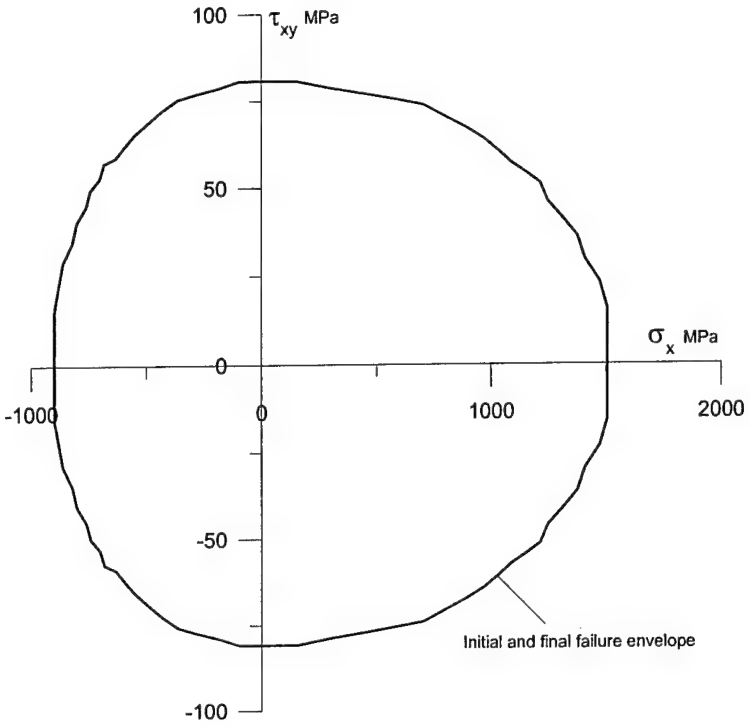

Fig. 5 *Failure envelope for a [0°] lamina made from T300/BSL914C under biaxial, σ_x/τ_{xy}, load.*

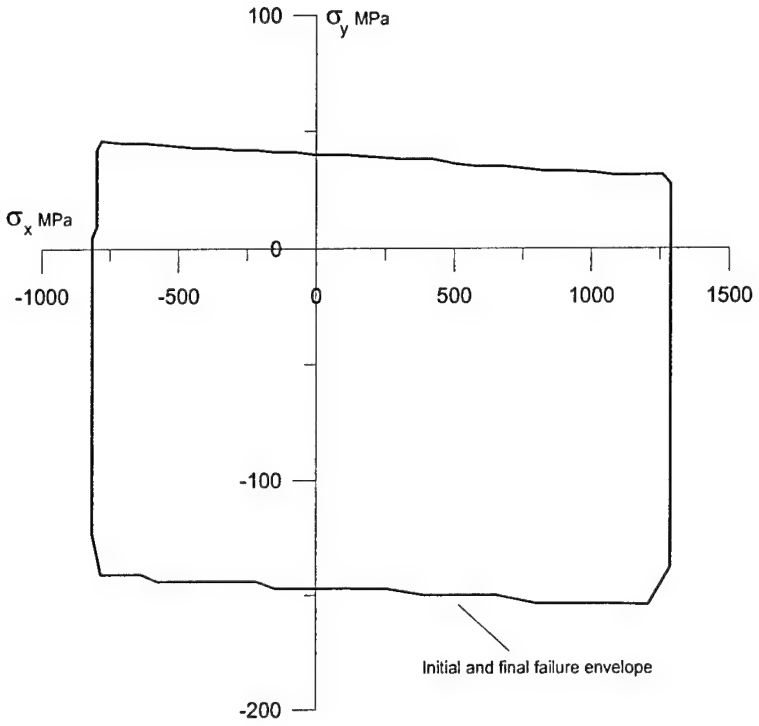

Fig. 6 *Failure envelope for a [0°] lamina made from E-glass/MY750/HT917/DY063 under biaxial, σ_y/σ_x, load.*

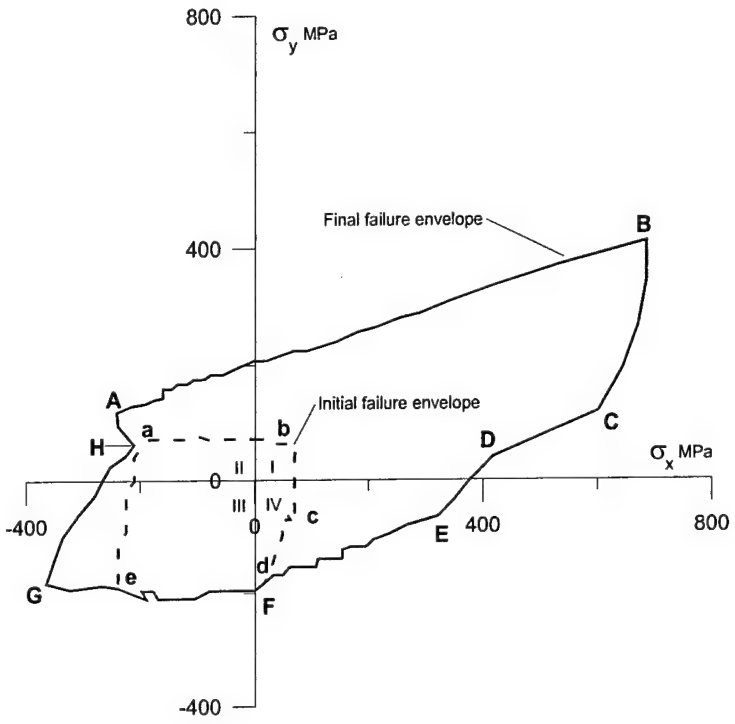

Fig. 7 *Failure envelope for a [90°/±30°]$_S$ laminate made from E-glass/LY556/HT907 /DY063 under biaxial, σ_y/σ_x, load.*

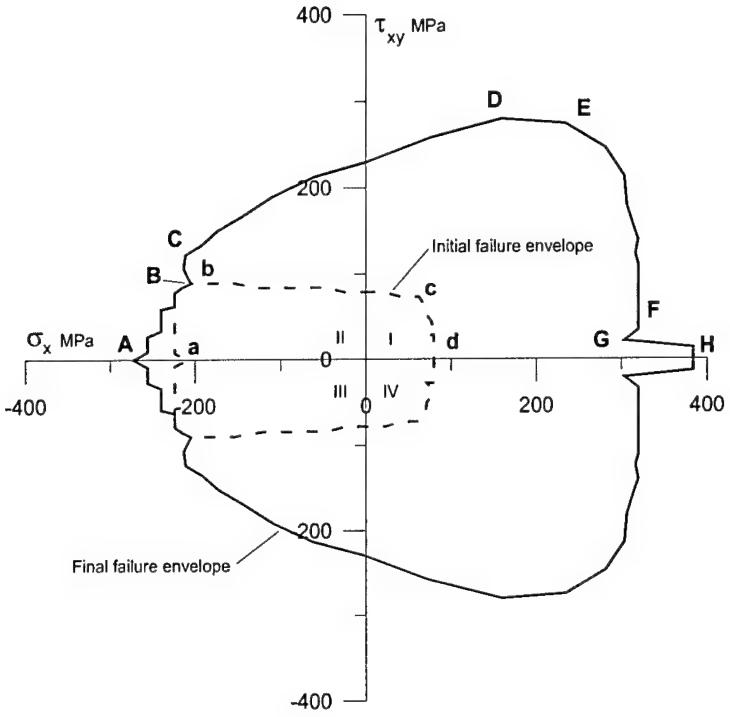

Fig. 8 *Failure envelope for a [90°/±30°]$_S$ laminate made from E-glass/LY556/HT907 /DY063 under biaxial, σ_x/τ_{xy}, load.*

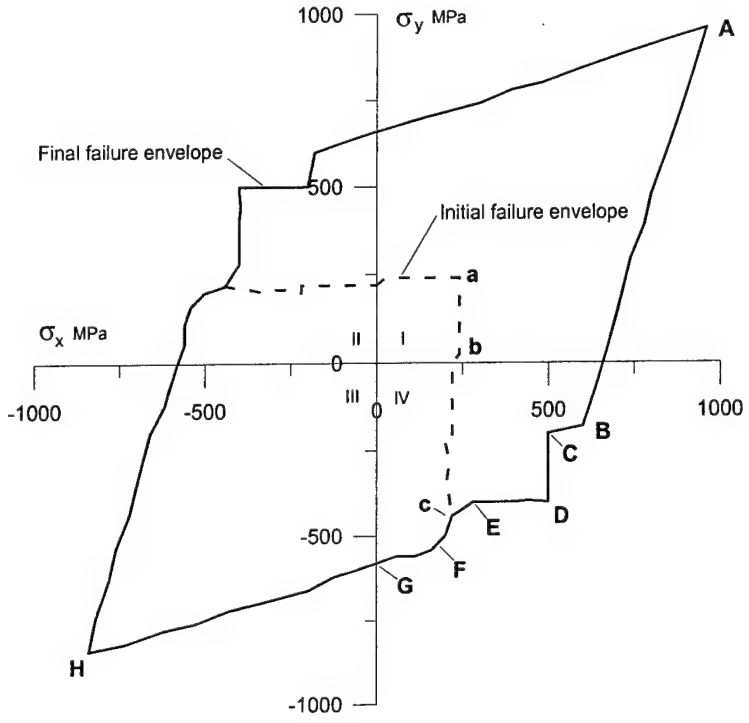

Fig. 9 *Failure envelope for a $[0°/\pm 45°/90°]_S$ laminate made from AS4/3501-6 under biaxial, σ_y/σ_x, load.*

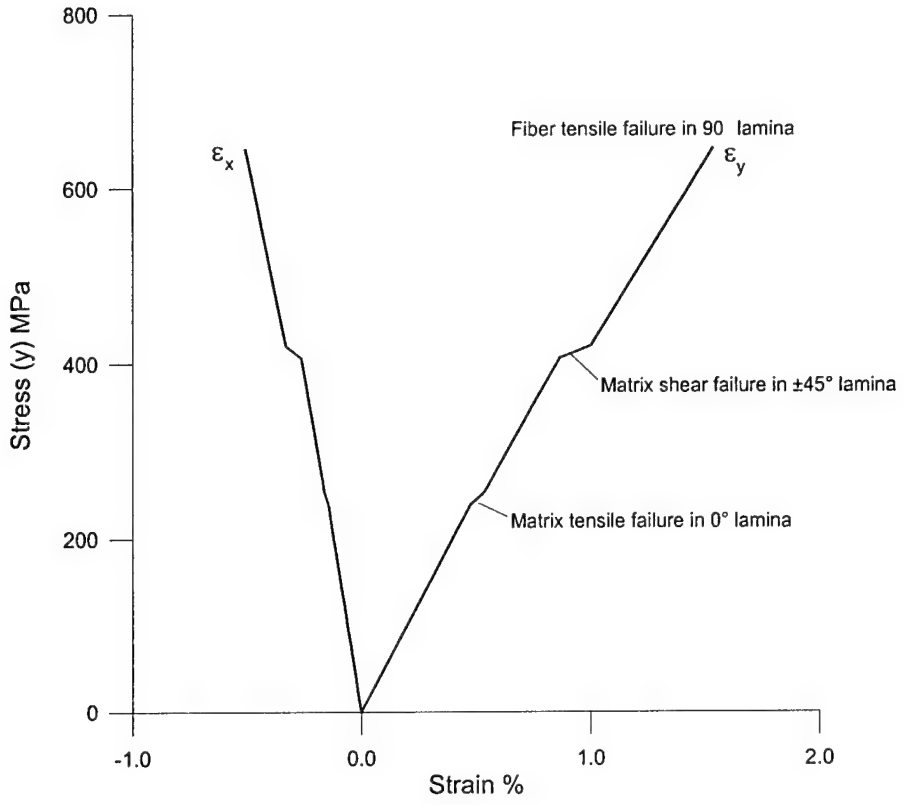

Fig. 10 *Stress/strain curves for a* $[0°/\pm45°/90°]_S$ *laminate made from AS4/3501-6 under uniaxial tension load* $\sigma_y/\sigma_x = 1/0$.

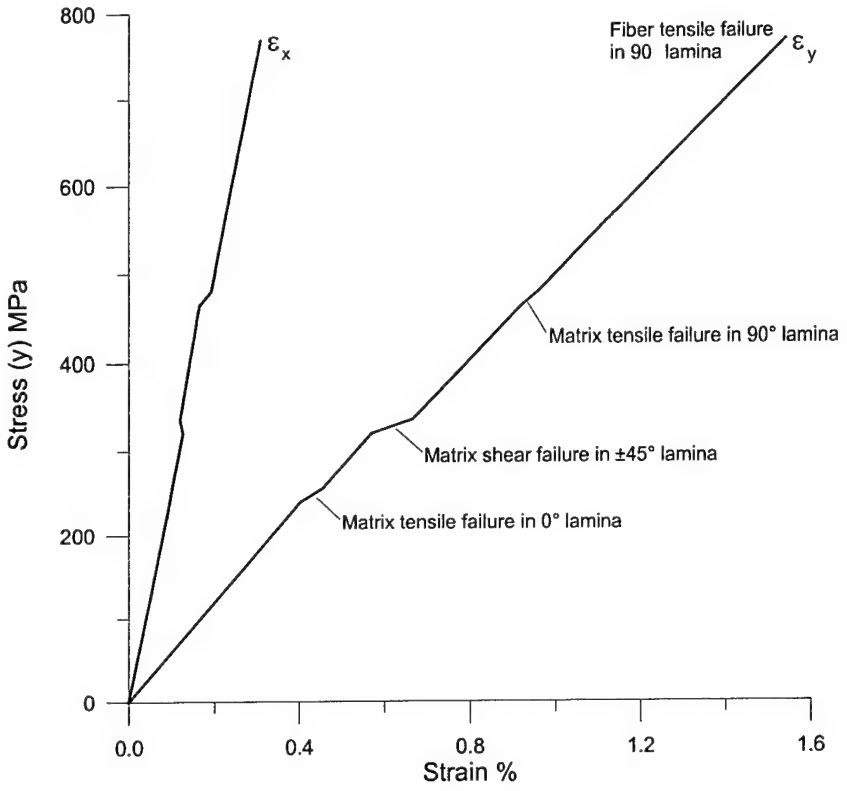

Fig. 11 *Stress/strain curves for a [0°/±45°/90°]$_S$ laminate made from AS4/3501-6 under biaxial tension load σ_y/σ_x = 2/1.*

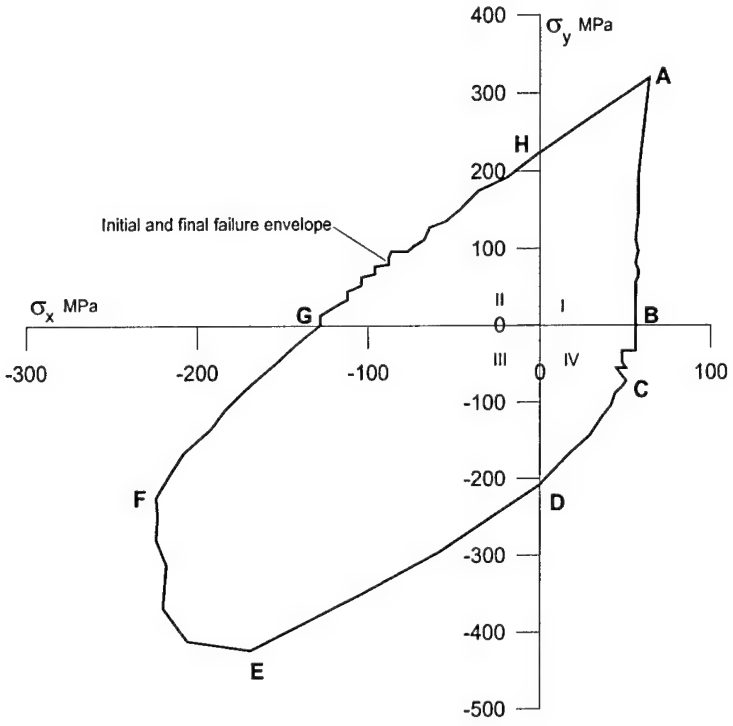

Fig. 12 *Failure envelope for a* $[\pm 55^\circ]_S$ *laminate made from E-glass/MY750/HT917 /DY063 under biaxial,* σ_y/σ_x*, load.*

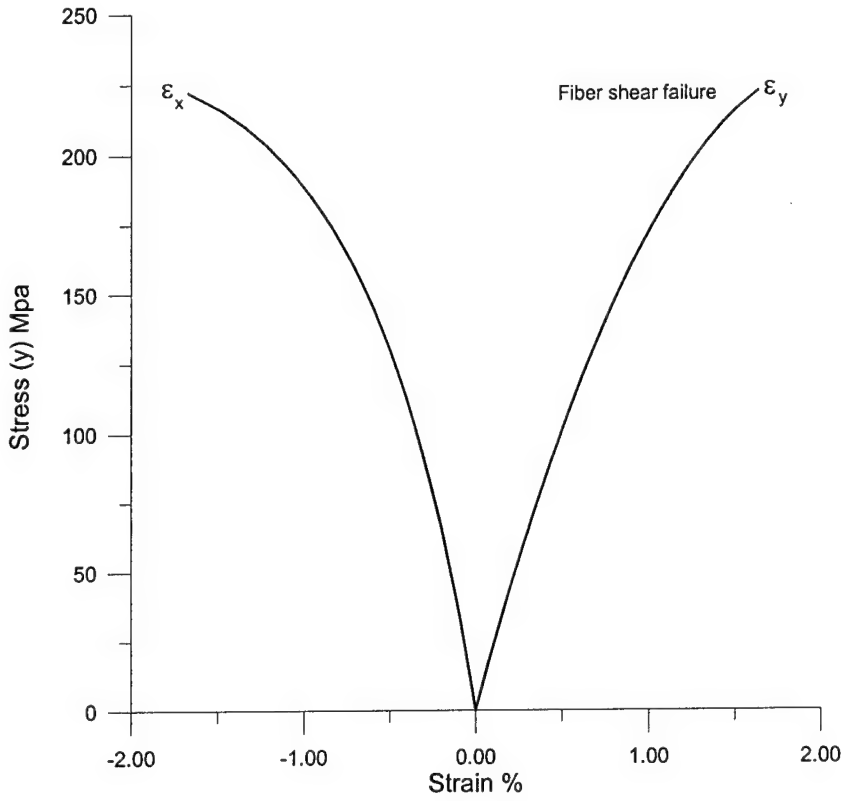

Fig. 13 *Stress/strain curves for a $[\pm 55\,^{\circ}]_S$ laminate made from E-glass/MY750/HT917 /DY063 under uniaxial tension load σ_y/σ_x = 1/0.*

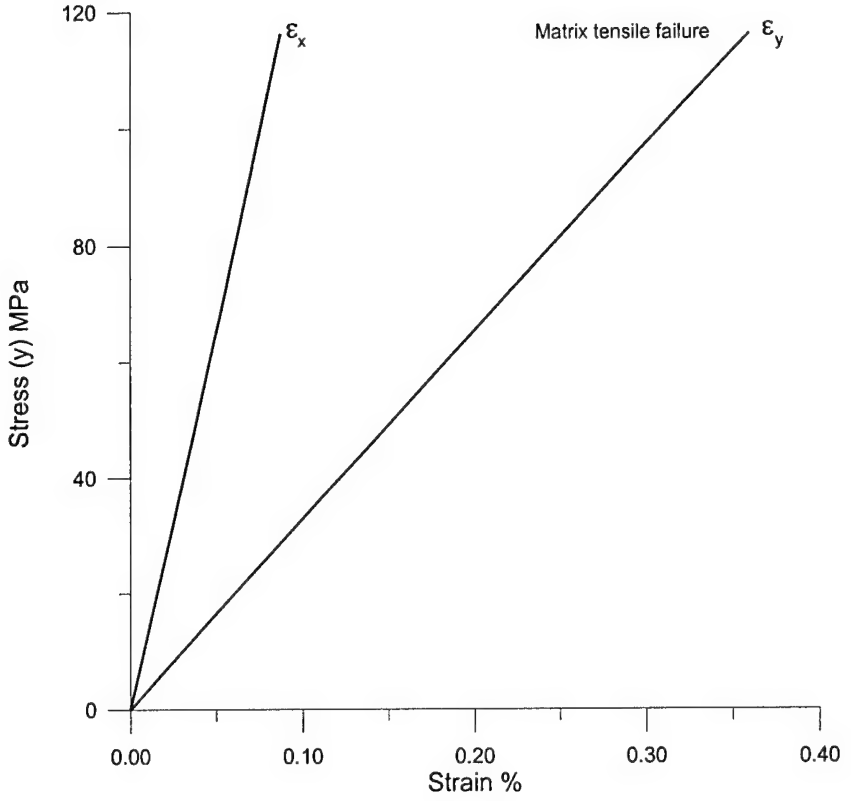

Fig. 14 *Stress/strain curves for a* $[\pm 55\,^{\circ}]_S$ *laminate made from E-glass/MY750/HT917 /DY063 under uniaxial tension load* $\sigma_y/\sigma_x = 2/1$.

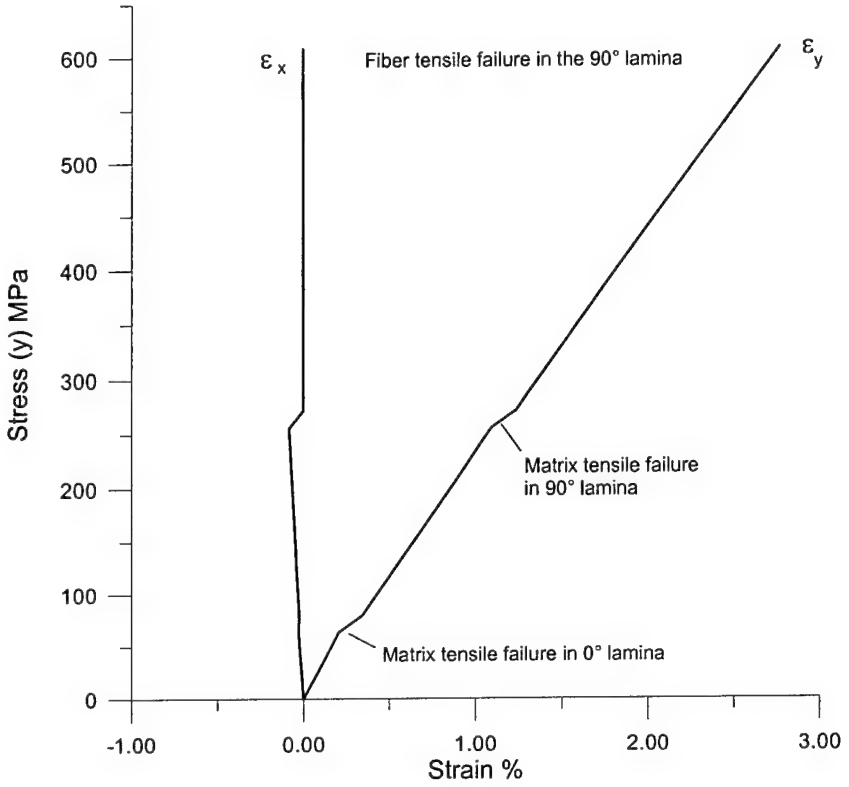

Fig. 15 *Stress/strain curves for a [0°/90°/0°] laminate made from E-glass/MY750/HT917/DY063 under uniaxial tension load* $\sigma_y/\sigma_x = 1/0$.

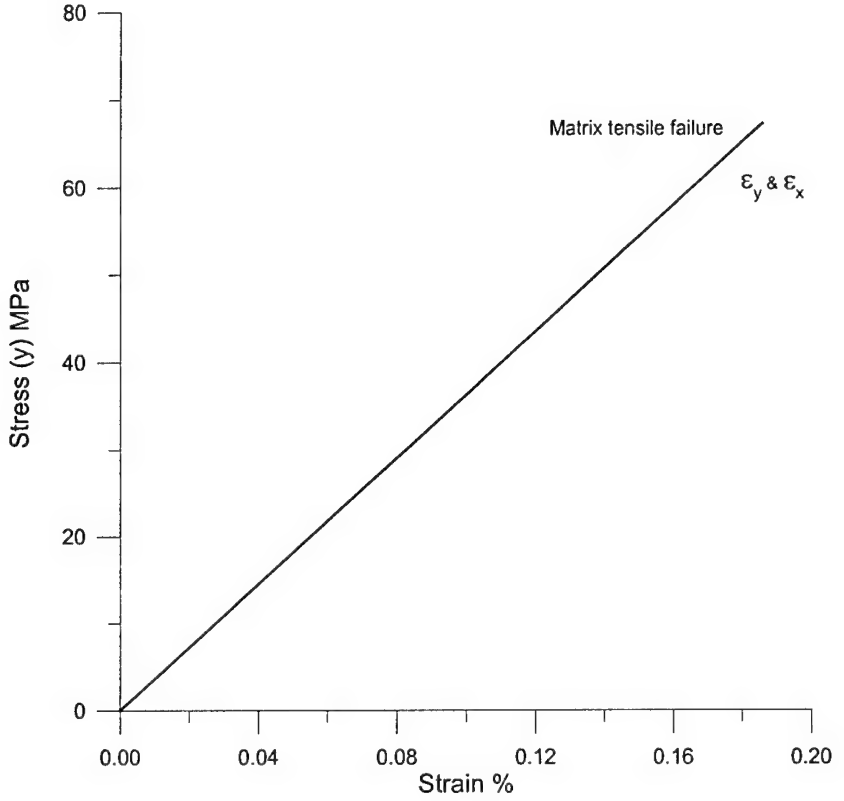

Fig. 16 *Stress/strain curves for a $[\pm 45\,^{\circ}]_S$ laminate made from E-glass/MY750/HT917 /DY063 under biaxial load σ_y/σ_x = 1/1.*

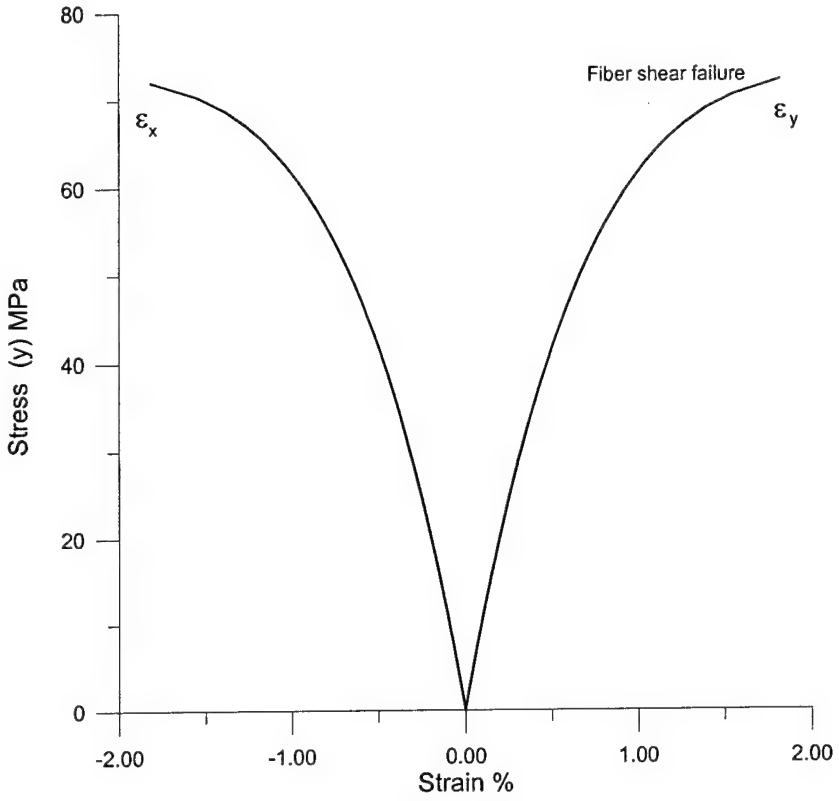

Fig. 17 *Stress/strain curves for a $[\pm 45\,^{\circ}]_S$ laminate made from E-glass/MY750/HT917 /DY063 under biaxial load σ_y/σ_x = 1/-1.*

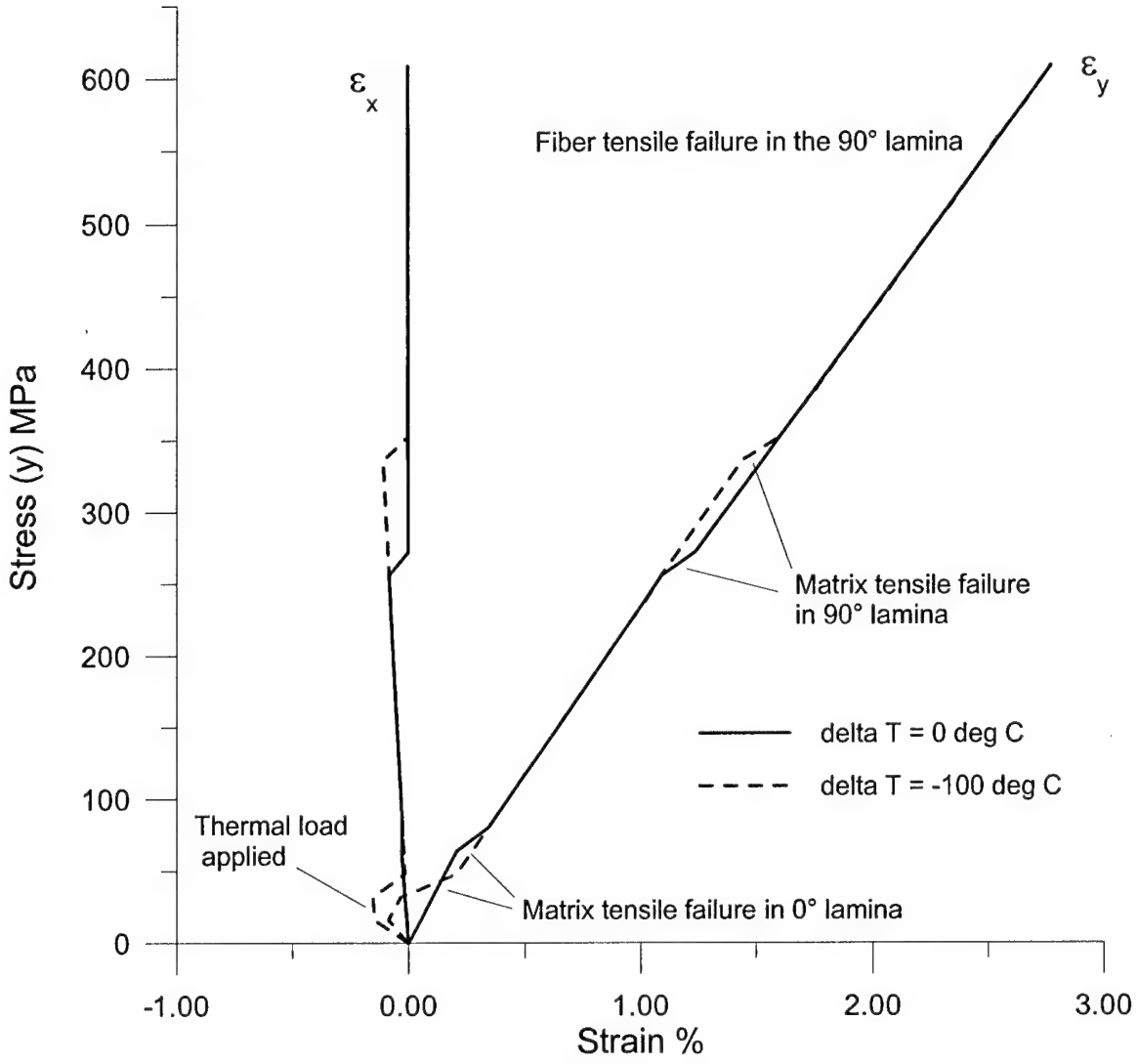

Fig. 18 *Stress/strain curves for a [0°/90°/0°] laminate made from E-glass/MY750/HT917 /DY063 under uniaxial tension load σ_y/σ_x = 1/0 and ΔT = -100°C*

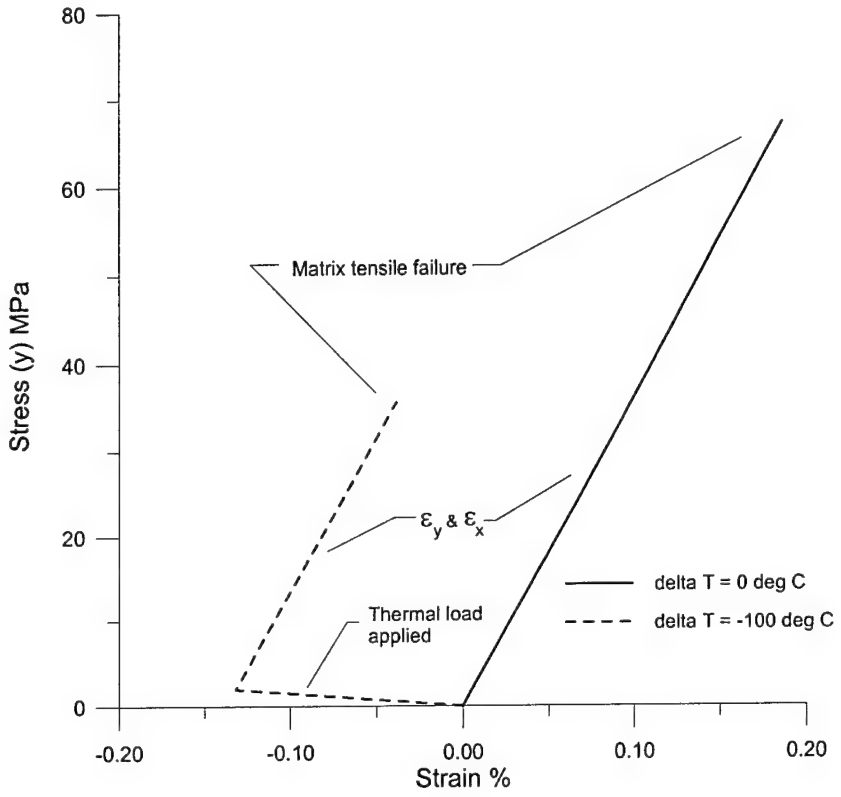

Fig. 19 *Stress/strain curves for a $[\pm 45\,^{\circ}]_S$ laminate made from E-glass/MY750/HT917 /DY063 under biaxial tension load σ_y/σ_x = 1/1 and ΔT = -100 °C.*

Matrix	E_m (GPa)	G_m (GPa)	ν_m	α_m (10^{-6}/°C)
3501-6	4.50	1.68	0.340	35
BSL914C	4.50	1.68	0.340	35
LY556/HT907/DY063	4.95	1.83	0.355	52
MY750/HY917/DY063	4.85	1.78	0.360	49

Table 1 *Matrix elastic constants calculated from micromechanics.*

Fiber	E_{11f} (GPa)	E_{22f} (GPa)	G_{12f} (GPa)	G_{23f} (GPa)	ν_{12f}	ν_{23f}	α_{11f} (10^{-6}/°C)	α_{22f} (10^{-6}/°C)
AS4	207.5	25.0	95.0	9.20	0.240	0.359	-1.7	15
T300	227.0	25.0	28.0	9.50	0.245	0.316	-1.7	15
E-glass 21xK43 Gevetex	83.2	83.2	33.5	33.5	0.240	0.240	6.9	6.9
Silenka E-glass 1200tex	73.0	73.0	29.6	29.6	0.235	0.235	6.6	6.6

Table 2 *Fiber elastic constants calculated from micromechanics.*

Matrix	$^{+}S_{22m}$ (MPa)	$^{-}S_{22m}$ (MPa)	$^{+22}S_{33m}$ (MPa)	$^{-22}S_{33m}$ (MPa)	S_{12m} (MPa)
3501-6	42.3	-176.3	5.52	-23.0	49.54
BSL914C	23.2	-172.2	2.73	-20.2	50.8
LY556/HT907 /DY063	27.3	-88.9	4.26	-13.9	44.9
MY750/HY917 /DY063	31.5	-114.3	4.63	-16.8	46.3

Table 3 *Matrix strengths calculated from micromechanics.*

Fiber	$^{+}S_{11f}$ (MPa)	$^{-}S_{11f}$ (MPa)	S_{12f} (MPa)
AS4	3202.	-2431.	101.
T300	2466.	-1480.	105.
E-glass 21xK43 Gevetex	1772.	-886.	93.0
Silenka E-glass 1200tex	2040.	-1275.	95.2

Table 4 *Fiber strengths calculated from micromechanics*

Composite	B_0 (Pa)	B_1 (Pa)	B_2 (Pa)	h_1	h_2
AS4/3501-6	3.31E+14	-1.09E+14	4.39E+14	-0.0536	-0.0132
T300/BSL914C	1.64E+11	-1.51E+8	-1.63E+11	-43.7	0.00654
E-glass/ LY556/HT907/DY063	5.76E+10	-9.51E+7	-5.75E+10	-71.9	0.00706
E-glass MY750/HY917/DY063	2.69E+10	-9.961E+7	-2.68E+10	-63.1	0.0161

Table 5 *Nonlinear shear curve fit parameters.*

Point	Lamina	Primary term	Secondary term	Failure mode
a	±30	$K_{3m}I_{3m} = 1.0$	$K_{4m}I_{4m} = 0.0$	Matrix - tension
b	90	$K_{3m}I_{3m} = 1.0$	$K_{4m}I_{4m} = 0.0$	Matrix - tension
c	90	$K_{3m}I_{3m} = 1.0$	$K_{4m}I_{4m} = 0.0$	Matrix - tension
d	±30	$K_{3m}I_{3m} = 0.66$	$K_{4m}I_{4m} = 0.34$	Matrix - comp/shear
e	90	$K_{3m}I_{3m} = 1.0$	$K_{4m}I_{4m} = 0.0$	Matrix - compression

Table 6 *Initial E-glass/LY55/HT907/DY063 failure envelope summary for a* $[90/\pm30]_S$ *laminate under biaxial,* σ_y/σ_x*, load.*

Point	Lamina	Primary term	Secondary term	Failure mode
A	30	$K_{4f}I_{4f} = 0.77$	$K_{1f}I_{1f} = 0.33$	Fiber - comp/shear
B	90	$K_{1f}I_{1f} = 1.0$	$K_{4f}I_{4f} = 0.0$	Fiber - tension
C	±30	$K_{1f}I_{1f} = 0.78$	$K_{4f}I_{4f} = 0.22$	Fiber - tension/shear
D	90	$K_{1f}I_{1f} = 1.0$	$K_{4f}I_{4f} = 0.0$	Fiber - compression
E	90	$K_{1f}I_{1f} = 1.0$	$K_{4f}I_{4f} = 0.0$	Fiber - compression
	±30	$K_{4f}I_{4f} = 0.83$	$K_{1f}I_{1f} = 0.17$	Fiber - shear/tension
F	±30	$K_{3m}I_{3m} = 0.66$	$K_{4m}I_{4m} = 0.34$	Matrix - comp/shear
	90	$K_{1f}I_{1f} = 1.0$	$K_{4f}I_{4f} = 0.0$	Fiber - compression
G	±30	$K_{3m}I_{3m} = 0.97$	$K_{4m}I_{4m} = 0.03$	Matrix - compression
	90	$K_{1f}I_{1f} = 1.0$	$K_{4f}I_{4f} = 0.0$	Fiber - compression
H	90	$K_{3m}I_{3m} = 1.0$	$K_{4m}I_{4m} = 0.0$	Matrix - compression
	±30	$K_{4f}I_{4f} = 0.71$	$K_{4f}I_{4f} = 0.29$	Fiber - shear/comp

Table 7 *Final E-glass/LY55/HT907/DY063 failure envelope summary for a [90°/±30°]$_S$ laminate under biaxial, σ_y/σ_x, load.*

Point	Lamina	Primary term	Secondary term	Failure mode
a	90	$K_{3m}I_{3m} = 1.0$	$K_{4m}I_{4m} = 0.0$	Matrix - compression
b	90	$K_{3m}I_{3m} = 0.72$	$K_{4m}I_{4m} = 0.28$	Matrix - comp/shear
	-30	$K_{3m}I_{3m} = 0.95$	$K_{4m}I_{4m} = 0.05$	Matrix - tension/shear
c	-30	$K_{3m}I_{3m} = 1.0$	$K_{4m}I_{4m} = 0.0$	Matrix - tension
d	90	$K_{3m}I_{3m} = 1.0$	$K_{4m}I_{4m} = 0.0$	Matrix - tension

Table 8 *Initial E-glass/LY55/HT907/DY063 failure envelope summary for a [90°/±30°]$_S$ laminate under biaxial, σ_x/σ_{xy}, load.*

Point	Lamina	Primary term	Secondary term	Failure mode
A	+30	$K_{f4}I_{f4} = 0.54$	$K_{1f}I_{1f} = 0.46$	Fiber - shear/comp
B	90	$K_{3m}I_{3m} = 0.72$	$K_{4m}I_{4m} = 0.28$	Matrix - comp/shear
	-30	$K_{3m}I_{3m} = 0.95$	$K_{4m}I_{4m} = 0.05$	Matrix - tension
	-30	$K_{1f}I_{1f} = 0.86$	$K_{4f}I_{4f} = 0.14$	Fiber - comp/shear
	+30	$K_{4f}I_{4f} = 0.98$	$K_{1f}I_{1f} = 0.02$	Fiber - shear
C	-30	$K_{1f}I_{1f} = 1.0$	$K_{4f}I_{4f} = 0.0$	Fiber - compression
	90	$K_{4f}I_{4f} = 0.91$	$K_{1f}I_{1f} = 0.08$	Fiber - shear/tension
	+30	$K_{4f}I_{4f} = 1.0$	$K_{1f}I_{1f} = 0.0$	Fiber - shear
D	-30	$K_{1f}I_{1f} = 1.0$	$K_{4f}I_{4f} = 0.0$	Fiber - tension
E	+30	$K_{1f}I_{1f} = 0.95$	$K_{4f}I_{4f} = 0.05$	Fiber - tension
F	+30	$K_{4m}I_{4m} = 0.72$	$K_{3m}I_{3m} = 0.28$	Fiber - shear/tension
G	-30	$K_{4m}I_{4m} = 0.61$	$K_{3m}I_{3m} = 0.39$	Matrix - tension/shear
	+30	$K_{4f}I_{4f} = 0.77$	$K_{1f}I_{1f} = 0.23$	Fiber - shear/tension
H	+30	$K_{4f}I_{4f} = 0.77$	$K_{1f}I_{1f} = 0.23$	Fiber - shear/tension
	90	$K_{1f}I_{1f} = 1.0$	$K_{4f}I_{4f} = 0.0$	Fiber - tension

Table 9 *Final E-glass/LY55/HT907/DY063 failure envelope summary for a [90°/±30°]$_S$ laminate under biaxial, σ_x/σ_{xy}, load.*

Point	Lamina	Primary term	Secondary term	Failure mode
a	All	$K_{3m}I_{3m} = 1.0$	$K_{4m}I_{4m} = 0.0$	Matrix - tension
b	90	$K_{3m}I_{3m} = 1.0$	$K_{4m}I_{4m} = 0.0$	Matrix - tension
c	90	$K_{3m}I_{3m} = 1.0$	$K_{4m}I_{4m} = 0.0$	Matrix - tension

Table 10 *Initial AS4/3501-6 failure envelope summary for a [0°/90°/±45°]$_S$ laminate under biaxial, σ_y/σ_x, load.*

Point	Lamina	Primary term	Secondary term	Failure mode
A	All	$K_{1f}I_{1f} = 1.0$	$K_{4f}I_{4f} = 0.0$	Fiber - tension
B	0	$K_{1f}I_{1f} = 1.0$	$K_{4f}I_{4f} = 0.0$	Fiber - tension
	90	$K_{1f}I_{1f} = 1.0$	$K_{4f}I_{4f} = 0.0$	Fiber - tension
	±45	$K_{4f}I_{4f} = 0.88$	$K_{1f}I_{1f} = 0.22$	Fiber - shear/tension
C	±45	$K_{4f}I_{4f} = 0.98$	$K_{1f}I_{1f} = 0.02$	Fiber - shear/tension
D	0	$K_{1f}I_{1f} = 1.0$	$K_{4f}I_{4f} = 0.0$	Fiber - tension
	90	$K_{1f}I_{1f} = 1.0$	$K_{4f}I_{4f} = 0.0$	Fiber - compression
E	±45	$K_{4f}I_{4f} = 1.0$	$K_{1f}I_{1f} = 0.0$	Fiber - shear
	90	$K_{1f}I_{1f} = 1.0$	$K_{4f}I_{4f} = 0.0$	Fiber - compression
F	90	$K_{1f}I_{1f} = 1.0$	$K_{4f}I_{4f} = 0.0$	Fiber - compression
	±45	$K_{4f}I_{4f} = 0.75$	$K_{1f}I_{1f} = 0.25$	Fiber - shear/comp
G	90	$K_{1f}I_{1f} = 1.0$	$K_{4f}I_{4f} = 0.0$	Fiber - compression
	±45	$K_{4f}I_{4f} = 0.66$	$K_{1f}I_{1f} = 0.34$	Fiber - shear/comp
H	All	$K_{1f}I_{1f} = 1.0$	$K_{4f}I_{4f} = 0.0$	Fiber - compression

Table 11 *Final AS4/3501-6 failure envelope summary for a $[0°/90°/\pm45°]_S$ laminate under biaxial, σ_y/σ_x, load.*

Point	Lamina	Primary term	Secondary term	Failure mode
A	±55	$K_{3m}I_{3m} = 1.0$	$K_{4m}I_{4m} = 0.0$	Matrix - tension
B	±55	$K_{3m}I_{3m} = .90$	$K_{4m}I_{4m} = 0.10$	Matrix - tension/shear
C	±55	$K_{3m}I_{3m} = 0.62$	$K_{4m}I_{4m} = 0.38$	Matrix - tension/shear
D	±55	$K_{4m}I_{4m} = 0.79$	$K_{3m}I_{3m} = 0.21$	Matrix - shear/tension
	±55	$K_{4f}I_{4f} = 0.86$	$K_{1f}I_{1f} = 0.14$	Fiber - shear/comp
E	±55	$K_{4f}I_{4f} = 0.61$	$K_{1f}I_{1f} = 0.39$	Fiber - shear/comp
F	±55	$K_{3m}I_{3m} = 0.87$	$K_{4m}I_{4m} = 0.13$	Matrix - comp/shear
G	±55	$K_{3m}I_{3m} = 0.69$	$K_{4m}I_{4m} = 0.31$	Matrix - comp/shear
H	±55	$K_{4f}I_{4f} = 0.96$	$K_{1f}I_{1f} = 0.04$	Fiber - shear/tension

Table 12 *E-glass/MY750/HT917/DY063 failure envelope summary for a $[\pm55°]_S$ laminate under biaxial, σ_y/σ_x, load.*

Component	Strength (MPa)	
	$\Delta T = 0°C$	$\Delta T = -100°C$
${}^{+}S_{11f}$	2040	2040
${}^{-}S_{11f}$	-1275	-1275
${}^{+}S_{22m}$	31.5	42.0
${}^{-}S_{22m}$	-114.3	-103.8
${}^{+22}S_{33m}$	4.63	15.09
${}^{-22}S_{33m}$	-16.8	-6.3

Table 13 *Effect of ΔT on constituent normal strengths for E-glass /MY750/HY917/DY063.*

Laminate	Lamina Matrix Stresses (MPa)		
	σ_{11m}	σ_{22m}	σ_{33m}
$[0°]_N$	27.1	10.5	10.5
$[\pm 15°]_S$	26.9	13.0	11.2
$[\pm 30°]_S$	28.4	19.5	12.5
$[\pm 45°]_S$	30.5	24.7	12.5

Table 14 *Thermally induced matrix stresses for ΔT = -100°C in each lamina of selected E-glass /MY750/HY917/DY063 laminates.*

Laminate	Strength (MPa)	
	$\Delta T = 0°C$	$\Delta T = -100°C$
$[\pm 45°]_S$	68.8	38.4
[0°/90°/0°]	624.	624.

Table 15 *Effect of ΔT on ultimate strength for E-glass /MY750/HY917/DY063 laminates under uniaxial load.*

[1] Aboudi, J., "Micromechanical Analysis of the Strength of Unidirectional Fiber Composites," *Composites Science and Technology,* 1988, Vol. 33, 79

[2] Pecknold, D.A. and S. Rahman, "Application of a New Micromechanics-Based Homogenization Technique for Nonlinear Compression of Thick-Section Laminates," *Compression Response of Composite Structures, ASTM STP 1185,* S.E. Groves and A.L. Highsmith, Eds., American Society for Testing and Materials, Philadelphia, 1994, 34.

[3] Rahman, S., and D.A. Pecknold, Micromechanics-Based Analysis of Fiber-Reinforced Laminated Composites, Civil Engineering Studies, UILU-ENG-92-2012, Department of Civil Engineering , University of Illinois, Urbana-Champaign, Sept 1992

[4] Kwon, Y.W., and J.M. Berner, "Micromechanics model for Damage and Failure Analyses of Laminated Fibrous Composites", *Engineering Fracture Mechanics,* 1995, Vol. 52, No. 2, 231

[5] Mayes, J.S., "Micromechanics Based Failure Analysis of Composite Structural Laminates," Naval Surface Warfare Center, Carderock Division Report, NSWCCD-65-TR–1999/15, September 1999

[6] Garnich M.R. and A.C. Hansen, "A Multicontinuum Theory for Thermal-Elastic Finite Element Analysis of Composite Materials, *Journal of Composite Materials*, 1997, Vol. 31, No. 1

[7] M.R. Garnich and A.C. Hansen, "A Multicontinuum Approach to Structural Analysis of Linear Viscoelastic Composite Materials, *Journal of Applied Mechanics*, Vol. 64, 1997, 795

[8] Agarwal, B.D. and L.J. Broutman, *Analysis and Performance of Fiber Composites*, 2nd Ed., John Wiley & Sons, New York, 1990

[9] Hill, R., "Theory of Mechanical Properties of Fibre Reinforced Materials - I. Elastic Behaviour," J. Mech. Phy. Solids, Vol. 12, pp199-212, 1964

[10] Garnich, M. R., 1996, *A Multicontinuum Theory for Structural Analysis of Composite Materials*, Ph.D. Dissertation, University of Wyoming.

[11] Brockenbrough, J.R., S. Suresh, & H.A. Wienecke, "*Deformation of Metal Matrix Composites with Continuous Fibers: Geometrical Effects of Fiber Distribution and Shape*", Acta Metallic Material, 1992

[12] Soden, P.D., Hinton, M.J. and Kaddour, A.S., "Lamina Properties, Lay-up Configuration and Loading Conditions for a Range of Fibre-Reinforced Composite Laminates," *Composites Science and Technology*, 1998, Vol. 58, No. 7, 1011

[13] Gibson, R.F. "Strength of a Continuous Fiber-Reinforced Lamina," in Principles of Composite Material Mechanics, McGraw-Hill, New York, 1994, 108

[14] Nahas, M. N., "Survey of Failure and Post-Failure Theories of Laminated Fiber-Reinforced Composites," *Journal of Composites Technology and Research,* Vol. 8, 1986, pp. 138-153.

[15] Gol'denblat, I. and Kopnov, V.A., "Strength of Glass Reinforced Plastics in the Complex Stress State," Mekhanika Polimerov, 1965, Vol. 1, 70, English translation: Polymer Mechanics, 1966, Vol. 1, 54

[16] Tsai, S.W. and Wu, E.M., "A General Theory of Strength for Anisotropic Materials," *Journal of Composite Materials*, 1971, Vol. 5, 58

[17] Hoffman, O., "The Brittle Strength of Orthotropic Materials," *Journal of Composite Materials*, 1967, Vol. 1,. 200

[18] Hashin, Z., "Failure Criteria for Unidirectional Fiber Composites," *Journal of Applied Mechanics*, 1980, Vol. 47, 329

[19] Hansen, A.C., D.M. Blackketter, and D.E. Walrath, "An Invariant-Based Flow Rule for Anisotropic Plasticity Applied to Composite Materials," *Journal of Applied Mechanics,* 1991, Vol. 58, 881

[20] Pipes, R.B., and B.W. Cole, "On the Off-Axis Strength Test for Anisotropic Materials," *Journal of Composite Materials*, 1973, Vol. 7, 246

[21] Narayanaswami, R., and H.M. Adelman, "Evaluation of the Tensor Polynomial and Hoffman Strength Theories for Composite Materials," *Journal of Composite Materials*, 1977, Vol. 11, 366

[22] Mayes, J. S., *Multicontinuum Failure Analysis of Composite Structural Laminates*, Ph.D. Dissertation, University of Wyoming, 1999

[23] Gipple, K. and E.T. Camponeschi, "The Influence of Material Nonlinearity and Microstructural Damage on Inplane Shear Response of Carbon/epoxy Composites", *Advanced Composites Letters*, 1992, Vol. 1 No. 1, 9.

[24] Hinton, M.J. and P.D., Soden, "Predicting Failure in Composite Laminates: The Background of the Exercise," *Composites Science and Technology*, 1998, Vol. 58, No. 7, 1001